THE STRUCTURAL AND FOLDING CHARACTERISTICS OF THE PLASMID-ENCODED TOXIN FROM ENTEROAGGREGATIVE *ESCHERICHIA COLI*

by

PATRICIA ANN SCAGLIONE
B.S. University of Central Florida, 2006

A dissertation submitted in partial fulfillment of the requirements
for the degree of Master of Science
in the Department of Molecular Biology and Microbiology
in the College of Medicine
at the University of Central Florida
Orlando, Florida

Fall Term
2008

Major Professor: Kenneth R. Teter

ABSTRACT

Plasmid-encoded toxin (Pet) from enteroaggregative *Escherichia coli* is a member of the autotransporter subfamily termed SPATE (serine protease autotransporters of *Enterobacteriaceae*). Autotransporters, which are the most common Gram-negative secreted virulence factors, contain three functional domains: an amino terminal leader sequence, a mature protein or passenger domain, and a carboxy-terminal β domain. The leader sequence targets the protein to the periplasmic space and the β domain then forms a β-barrel pore in the outer membrane of the bacterium which allows the passenger domain to enter the external milieu. In some cases the passenger domain is cleaved from the β-barrel at the extracellular surface to release a soluble toxin. This is thought to be a self-contained process that does not require chaperones or ATP for folding and export of the passenger domain.

Pet produces cytotoxic effects through cleavage of its target, the actin-binding protein α-fodrin. Pet is secreted into the extracellular environment, but its target lies within the cytosol. To reach its target, Pet moves from the cell surface to the ER where it triggers ER-associated degradation (ERAD) to enter the cytosol. ERAD is a normal cellular process in which improperly folded proteins are exported from the ER to the cytosol for degradation. Other toxins that utilize this pathway are AB toxins such as cholera toxin (CT) and ricin. The A subunits of these toxins are thermally unstable, and this facilitates their ERAD-dependent translocation into the cytosol. Pet, however, is not an AB toxin. We predict that thermal unfolding is not the mechanism Pet employs to exploit ERAD.

It was necessary to purify the toxin first in order to study the structural properties and ER export of Pet. Surprisingly, purified Pet eluted as two close peaks by size exclusion

chromatography. Both peaks were Pet as demonstrated through immunoblotting. The folding efficiency of autotransporters has not been extensively elucidated, and based on our purification results, we hypothesized that there is inefficiency in the folding of autotransporters, specifically Pet. A toxicity assay showed that Pet peak one did not display cytopathic activity while Pet peak two did. CD and fluorescence spectroscopy measurements also detected structural differences between the two variants of Pet and demonstrated that Pet peak one was an unfolded variant of Pet peak two. Native gel electrophoresis and biophysical measurements indicated that Pet peak one did not exist as a dimer or aggregate. Our results indicate there are two forms of Pet, and thus the folding process of autotransporters appears to be inherently inefficient.

Active Pet (peak two) was used for further biophysical measurements and biochemical assays. Circular dichroism and fluorescence spectroscopy showed that the secondary and tertiary structures of Pet are maintained at physiological temperature, 37°C. Thermal unfolding of Pet occurred at temperatures above 50°C. Fluorescence quenching of Pet was also performed and demonstrated that, at 37°C, there are solvent-exposed aromatic amino acids. The slight structural alterations to Pet at physiological temperature as well as the exposed hydrophobic residues could trigger ERAD. In addition, a modeled structure of Pet revealed a hydrophobic loop which is surface-exposed and a likely target for toxin-ERAD interactions. The data suggests that translocation of Pet mediated by ERAD can occur by a mechanism different from certain AB toxins. An open, hydrophobic conformation likely triggers ERAD, but may also contribute to poor folding.

ACKNOWLEDGMENTS

I am especially grateful to Dr. Navarro-Garcia for sending Pet for my research. Without the gift of the toxin none of this would have been possible. I owe an enormous debt to Dr. Kathleen Nemec for spending countless hours teaching me the foundation of performing biophysical measurements. Dr. Tatulian was instrumental in helping me analyze and understand the abstract concepts of biophysics. I'd like to give special thanks to Supriyo Ray for dedicating numerous Sunday's to helping me in the physics lab. I can't go without thanks my lab-mates: Shane Massey, Mike Taylor, Sandy Geden, and Dave Curtis for never making it a dull day. Most of all I would like to thank Dr. Teter for being such a great mentor, and providing me with support and guidance over the last two years. Of course, I am very blessed to have such a wonderful family, my mom and dad, whose endless love and support have shaped me into the women I am today. To the love of my life Paul, words cannot express how much you mean to me. Thanks for always standing by my side.

TABLE OF CONTENTS

LIST OF FIGURES

LIST OF ACRONYMS/ABBREVIATIONS

λ_{max}	maximum emission wavelength
CD	circular dichroism
CT	cholera toxin
DAEC	Diffusely adherent *Escherichia coli*
DT	diphtheria toxin
EAEC	Enteroaggregative *Escherichia coli*
EHEC	Enterohemorrhagic *Escherichia coli*
EIEC	Enteroinvasive *Escherichia coli*
EPEC	Enteropathogenic *Escherichia coli*
ER	endoplasmic reticulum
ERAD	ER-associated degradation
ETEC	Enterotoxigenic *Escherichia coli*
Hbp	Hemoglobin protease
IgA1	Immunoglobulin A1 protease
K_{SV}	Stern-Volmer constant
NaPi	sodium phosphate
pAA	aggregative adherence plasmid
Pet	plasmid-encoded toxin
PT	pertussis toxin
SPATE	serine protease autotransporters of Enterobacteriaceae
T_m	Transitions midpoint

CHAPTER ONE: INTRODUCTION

Overview

Plasmid-encoded toxin (Pet) from enteroaggregative *Escherichia coli* (EAEC) is a 104 kDa protein and a member of the autotransporter class of secreted proteins. Pet is a member of a subfamily of autotransporters termed SPATE (serine protease autotransporters of *Enterobacteriaceae*) which utilize a conserved serine protease motif to induce cytotoxicity. The cellular effects Pet produces are through cleavage of its target, the actin-binding protein α fodrin. Cell rounding, detachment from the epithelium, mucosal damage, and continual watery diarrhea all result from the loss of the organization of the actin cytoskeleton (Henderson, Hicks et al. 1999).

Pet is secreted into the extracellular environment, but its target lies within the cytosol. Pet traffics from the plasma membrane to the endoplasmic reticulum (ER), where it triggers the mechanism ER-associated degradation (ERAD) and exits the ER to reach its cytosolic target (Navarro-Garcia, Canizalez-Roman et al. 2001; Navarro-Garcia, Canizalez-Roman et al. 2007a). ERAD is a quality control mechanism that recognizes misfolded proteins in the ER and targets them through the protein-conducting channels to the cytosol where they may be degraded by the proteasome (Romisch 1999; Romisch 2005). ERAD has been implicated in Pet translocation, as Pet intoxication was hindered in ERAD deficient mutant CHO cell lines (Navarro-Garcia, Canizalez-Roman et al. 2007a).

Enteroaggregative *Escherichia coli*

The vast majority of *E. coli* are a part of our intestinal normal flora and are considered harmless. There are, however, some strains that are pathogenic due to the expression of certain virulence factors. To date, there are six pathogenic strains of *E. coli* linked to gastroenteritis: EAEC, enterotoxigenic (ETEC), enterohemorrhagic (EHEC), diffusely adherent (DAEC), enteropathogenic (EPEC), and enteroinvasive (EIEC) (Harrington, Dudley et al. 2006). In developing countries such as Mexico, Bangladesh, and Serbia, EAEC is responsible for significant numbers of cases of pediatric diarrhea. This emerging pathogen has also been implicated in persistent diarrhea in immunocomprimised patients as well as traveler's diarrhea. EAEC elicits two well-known cytopathic characteristics; production of mucous on the intestinal epithelium and damage of the mucosa through secretion of enterotoxins such as Pet (Eslava, Navarro-Garcia et al. 1998; Villaseca, Navarro-Garcia et al. 2000).

In 1985 EAEC was characterized by its ability to adhere to Hep-2 cells in an aggregative "stack brick" pattern when initiating pathogenesis in the ileum and large intestine. The factors responsible for this characteristic phenotype are maintained on a plasmid called aggregative adherence (pAA), which is necessary for the expression of AA fimbriae (Harrington, Dudley et al. 2006). Pet was identified through ammonium sulfate precipitation of supernatants from an EAEC strain that was isolated during an outbreak. The 104 kDa cytotoxin Pet is encoded on the 65-MDa AA plasmid (Navarro-Garcia, Eslava et al. 1998). Heat stable toxin-1 (EAST-1) is another virulence factor that is found on the same plasmid as Pet and the AA fimbriae. EAST-1 is a 116 kDa protein that is closely related to the enterotoxigenic *E. coli* (ETEC) heat-stable enterotoxin (ST), which is highly potent for short durations and increases levels of cyclic guanosine monophosphate (cGMP). ST was identified in the same manner as Pet. This protein,

EAST-1, does not produce enterotoxic symptoms, thus indicating that Pet is responsible for the observed toxic effects. Pet, when added alone to tissue samples, generated cell exfoliation and crypt abscesses in addition to mucus formation (Navarro-Garcia, Eslava et al. 1998). Pet also induced fluid accumulation and mucosal damage when injected into an ileal loop of a rat. Patients afflicted by certain strains of EAEC exhibit secretory stools without blood or polymorphonuclear cells indicating the involvement of a cytotoxin such as Pet (Henderson, Hicks et al. 1999). To better understand the emergence of EAEC as a human pathogen, it is important to examine Pet and other EAEC virulence factors (Harrington, Dudley et al. 2006).

Autotransporters

Pet from EAEC is a 104 kDa protein and a member of the autotransporter class of secreted proteins. Gram-negative bacteria may utilize five different secretion pathways (type I-V) to disseminate various virulence factors to their host. The type V secretion system is also referred to as autotransporter secretion. Several different pathogens produce autotransporter proteins, including *E. coli*, *Bordetella pertussis*, *Helicobacter pylori*, *Pseudomonas aeruginosa*, and *Yersinia pestis*. The term autotransporter came about because the protein domain that initiates translocation across the outer membrane is a part of the secreted protein prior to proteolysis. The first protein described to employ this mechanism was immunoglobulin A1 (IgA1) protease (Henderson, Navarro-Garcia et al. 1998). The autotransporter class all share a conserved structure consisting of thee domains: the amino-terminal signal sequence, the secreted passenger or mature protein, and the carboxy-terminal β-barrel domain. Despite the unifying organization of the autotransporters and a common β-helix motif in the passenger domain, autotransporters display various modes of action (Henderson and Nataro 2001).

The amino-terminal signal peptide is closely related to the type II secretion pathway in that the signal sequence is recognized in a Sec dependent manner. In the cytoplasm, SecB recognizes the nascent signal peptide and targets it to SecA which directly permits translocation. SecB is thought to play a role and acts as a chaperone to maintain the autotransporter in a state necessary for translocation. Functionally, the signal peptide initiates transport to the inner membrane where the Sec protein channel resides, and targets an autotransporter to the periplasm. The amino-terminal peptides of autotransporters have characteristic features: a positively charged N-domain, a neutral and hydrophobic H-domain, and a C-domain that contains a signal peptidase identification motif (Henderson, Navarro-Garcia et al. 1998). However, Pet's signal peptide is considerably long in comparison to other autotransporters. Pet's conserved N-terminal signal sequence contains an extended N-domain that adds to the length of the protein.

It is in the periplasmic space that the signal peptide is proteolytically cleaved from the nascent toxin (Henderson, Navarro-Garcia et al. 1998; Henderson, Navarro-Garcia et al. 2004). After export through the inner membrane autotransporters exist as an intermediate in the periplasm, where the proprotein is kept in an unfolded conformation, because if it folds then translocation will not occur. This was first demonstrated with IgA1 protease where a recombinant passenger domain with cysteines was created, and the disulfide bond formation resulted in inhibition of outer membrane translocation (Klauser, Kramer et al. 1993). Autotransporters have a lack of cysteine residues in the mature protein so that outer membrane translocation cannot be hindered by the formation of disulfide bonds. Controversies exist over whether there is a chaperone in the periplasmic space that protects the autotransporter from proteases or whether the autotransporter itself has chaperone capabilities (Henderson, Navarro-Garcia et al. 1998; Henderson, Navarro-Garcia et al. 2004).

The β-barrel domain is thought to form spontaneously in the outer membrane as first suggested by Pohlner *et al*. It is comprised of antiparallel β-sheets that are amphipathic in nature. The β-barrel pore is formed from an even number of transmembrane β-sheets and hydrogen bonds between the first and the last β-sheets. The core of the pore consists of hydrophobic residues which protrude into the lipid bilayer, and hydrophilic residues extend beyond the outer membrane into the extracellular environment (Henderson, Navarro-Garcia et al. 1998). The C-terminal domain of Pet was deemed necessary for translocation into the extracellular environment when, after truncation and expression, the recombinant toxin could not be located in the supernatant but was instead found to a greater extent in the periplasm (Eslava, Navarro-Garcia et al. 1998).

Secretion of the passenger domain through the outer membrane proceeds from C-terminus to N-terminus through the β-barrel pore. The diameter of the pore is about 2 nm, which suggests that the passenger domain must maintain an unfolded conformation in order for it to reach the external milieu (Henderson, Navarro-Garcia et al. 2004). In the case of hemoglobin protease (Hbp), it has recently been suggested that, while the protein may fold in the periplasm, it maintains a specific level of flexibility in order to pass through the outer membrane pore (Jong, ten Hagen-Jongman et al. 2007). The secretion of autotransporters does not require a proton gradient or ATP, and is therefore an energy-independent phenomenon (Junker, Schuster et al. 2006).

The fate of the autotransporter is determined once the mature protein reaches the surface of the bacterial cell. There are several events that can occur depending on the biological function of the passenger domain (Henderson and Nataro 2001). The mature protein may be cleaved but remain noncovalently associated with the β-domain as in the case of pertactin, an adhesin from

Bordetella pertussis. Also, the passenger domain may remain as an intact membrane-bound protein with the N-terminal domain protruding into the extracellular environment such as the adhesin Hia autotransporter from *Haemophilus influenzae*. Pet and extracellular serine protease plasmid-encoded (EspP), an autotransporter produced by enterohaemorrhagic *E. coli* O157, are proteolytically nicked from their β-barrel domains and secreted into the environment. Processing of the protein from the β-barrel pore still remains an issue of controversy. The cleavage event may be autocatalytic or result from another protease. It has been demonstrated that cleavage and secretion still occurs for autotransporters, specifically Pet, with a mutated serine protease motif, suggesting that there are proteases that aid in the processing event (Henderson, Navarro-Garcia et al. 2004). Cleavage of the native Pet protein occurs between residues N1018 and N1019, because mutation of these residues resulted in a bacterial surface coated with unprocessed toxin (Navarro-Garcia, Canizalez-Roman et al. 2001).

Serine Protease Autotransporters of Enterobacteriaceae (SPATE)

Pet is a member of a subfamily of autotransporters termed SPATE (serine protease autotransporters of *Enterobacteriaceae*) which utilize a conserved serine protease motif to induce cytotoxicity. The SPATE family virulence proteins are produced by *E. coli* and *Shigella* species and have been investigated since 1994 (Henderson, Navarro-Garcia et al. 2004). Temperature-sensitive hemagglutinin (Tsh), a protein secreted from avian *E. coli*, was the first SPATE to be discovered. Since then numerous SPATE proteins from pathogenic strains of *E. coli* have been described, including Pet, EspC (EPEC-secreted protein), EspP, and Sat (secreted autotransporter toxin from uropathogenic *E. coli*). *Shigella* species express three SPATE proteins: SepA (*Shigella* extracellular protein), and SigA (*Shigella* IgA-like protease homolog).

Pic (protein involved in intestinal colonization) has been identified in both species (Henderson and Nataro 2001; Henderson, Czeczulin et al. 1999). Sequence analysis of the *pet* gene demonstrated that Pet belongs to the SPATE autotransporter subfamily, which utilizes a conserved serine protease motif to induce cytotoxicity. The passenger domains of this family all share an evolutionary conserved sequence, GDSGSPL, which includes the active site serine residue (underlined) (Otto, Sijbrandi et al. 2005; Sui, Dutta et al. 2003). The serine protease motif of Pet has been shown to be necessary for the enterotoxic effects. This was demonstrated with a Pet mutant where the serine residue was mutated to an isoleucine residue (S260I) and no cytotoxic effect was observed when added to cells. In addition to the generated mutant, the cytotoxic effects of Pet were also inhibited by phenylmethylsulfonyl fluoride, a serine protease inhibitor. Although Pet S260I was unable to elicit a cytotoxic response it was still capable of being secreted into the extracellular milieu (Navarro-Garcia, Canizalez-Roman et al. 2001).

Despite the dissimilar functions and substrate specificities for all the SPATE proteins, they share quite a few features in common. For example, the serine protease is not involved in the autoprocessing event that occurs on the surface of the outer membrane. In addition, all SPATE proteins are similar in that they do not partake in IgA1 cleavage; have not been described in organisms that are nonpathogenic; are the predominant secreted protein of the pathogen; and elicit a strong immune response (Henderson, Navarro-Garcia et al. 2004; Otto, Sijbrandi et al. 2005).

Amino acid analysis showed Pet shared 58% overall identity and 83% similarity to EspP, 55% identity and 70% similarity with EspC and 44% identity and 60% similarity with SepA based on the provided sequences available in GenBank databases. The homology between these proteins is not uniform and there is more sequence identity displayed in the carboxy-terminal

domain. The *pet* gene encodes a 1,295 amino acid, 140 kDa proprotein that has a 6.71 isoelectric point. Pet was the first secreted autotransporter enterotoxin described (Eslava, Navarro-Garcia et al. 1998).

Pet: Cytoskeletal Disruption and Intestinal Damage

Intestinal mucosal damage produced by EAEC is due in whole to the presence of Pet. Pet intoxication results in extensive mucous release, shedding of cells, and crypt abscess formation. The injection of Pet into a rat ileal loop produced fluid accumulation, microvilli shortening, and necrosis of the mucosa (Villaseca, Navarro-Garcia et al. 2000). The cytotoxic and enterotoxic effects seen during EAEC intoxication are due to the breakdown α-fodrin, the intracellular target of Pet. Because Pet's intracellular target is a cytoskeletal protein that organizes to actin, its cytopathic effects result in cytoskeletal contraction and the disengagement of focal contacts (Canizalez-Roman and Navarro-Garcia 2003). The lack of an intact epithelium is lost due to cell rounding and detachment followed by continual watery diarrhea (Henderson, Hicks et al. 1999).

Fodrin is a ubiquitous protein that is implicated in connecting integral membrane proteins to actin filaments. Fodrin also plays a role with the organization of receptor domains and is involved at the plasma membrane with vesicle trafficking. Structurally, fodrin is rod-shaped and comprised of α and β subunits which come together to produce heterodimers. The heterodimers then form tetramers, and it is the tetramer that cross-links the ends of actin filaments (Canizalez-Roman and Navarro-Garcia 2003). Physiologically, the calcium-dependent proteolysis of fodrin by calpain I is part of many processes such as white blood cell and platelet activation, secretion, and neuronal synapses. Interestingly, calmodulin has been shown to coordinate the association of fodrin with actin, but in the presence of calpain I, calmodulin interferes with the tetramer

formation of fodrin (Harris and Morrow 1990). Upon cleavage by Pet, fodrin is distributed in the cell as aggregated membrane blebs which can be observed between one and three hours after the addition of Pet. The serine protease activity of Pet occurs in the calmodulin-binding domain between Methionine $(M)_{1198}$ and Valine $(V)_{1199}$ of α-fodrin, and is considered a region of protease hypersensitivity (Canizalez-Roman and Navarro-Garcia 2003). The diarrhoeal disease resulting from EAEC can be explained because α-fodrin forms a complex with the sodium channels of the intestinal epithelia (Zuckerman, Chen et al. 1999). The macromolecular complex formed prevents the reabsorption of sodium thus leading to diarrhea (Garty and Palmer 1997). The cytoskeletal effects generated by Pet are a result of fodrin proteolysis and the lack of actin interaction with cleaved protein (Canizalez-Roman and Navarro-Garcia 2003).

Intracellular Trafficking and Translocation of Pet in Host Cells

In order for intoxication of epithelial cells to occur Pet internalization is required. The cytopathic effects of Pet are first observed after two hours of incubation, which allows time for entry and translocation. The requirement of intracellular uptake was demonstrated through the observed effects of three chemical inhibitors: brefeldin A, chloroquine, and ammonium chloride. Brefeldin A blocks trafficking by causing the collapse of the Golgi stacks into the ER. Chloroquine and ammonium chloride affect vesicular trafficking through alkalinizing the endosomes and trans Golgi network (TGN). Pretreatment of HEp-2 cells with brefeldin A to inhibited Pet cytotoxicity, which indicates that Pet requires passage to or through the Golgi apparatus and is commonly associated with toxins that travel by retrograde transport to the ER (Navarro-Garcia, Canizalez-Roman et al. 2001). Chloroquine and ammonium chloride did not significantly effect Pet intoxication, suggesting that Pet does not utilize the acidic pH of the

endosomes to reach the cytosol. This is also common for toxins that travel to the ER such as diphtheria toxin (DT). There are, however, specific toxins that require the acidic pH of endosomes to translocate into the cytosol. Pet, a non-AB toxin, thus traffics in the same manner as some AB toxins such as cholera toxin (CT), ricin, Shiga toxin, and *Pseudomonas* exotoxin A. (Navarro-Garcia, Canizalez-Roman et al. 2001).

After the 104 kDa mature Pet protein is secreted by EAEC, it associates with the plasma membrane of the host cell and is eventually observed in epithelial cells. On the cell surface, Pet enters the cell through an unidentified receptor and is internalized via clathrin-mediated endocytosis (Navarro-Garcia, Canizalez-Roman et al. 2007b). The internalization of Pet is mediated by clathrin as shown by two mechanisms. The first mechanism provides evidence for clathrin-dependent endocytosis because it is blocked when cells are pretreated with monodansylcadaverine (MDC) (Navarro-Garcia, Canizalez-Roman et al. 2007b). MDC inhibits clathrin-dependent endocytosis by preventing the clustering of clathrin and thus clathrin-coated vesicle internalization (Rikihisa, Zhang et al. 1994). The second mechanism demonstrates that the uptake of Pet still occurred when the cells were pretreated with filipin, which binds cholesterol and inhibits caveolae vesicle formation. The results revealed by immunofluorescence that Pet was localized only on the outer surface of the cell, suggesting lipid rafts are not involved in Pet endocytosis. Pet was also found to interact with clathrin which was demonstrated by a co-immunoprecipitation assay (Navarro-Garcia, Canizalez-Roman et al. 2007b).

Intracellular traffic of Pet proceeds from the early endosomes to the Golgi apparatus, then from the Golgi to the ER. In the ER, Pet associates with the Sec61p translocon as demonstrated by colocalization and coimmunoprecipitation assays. It then enters the cytosol and can be detected in the cytosol of fractionated cells as an intact 104 kDa protein. Toxin translocation

into the cytosol often involves a quality control mechanism of the cell, ER-associated degradation (ERAD), which targets misfolded proteins in the ER for proteasomal degradation in the cytosol. Pet translocation has also been implicated in ERAD because Pet intoxication was inhibited in ERAD deficient cell lines. Cells treated with a proteasomal inhibitor, N-acetyl-Leu-Leu-Norleu-Al (ALLN), were also more sensitive to Pet, suggesting that translocation of Pet to the cytosol is prone to degradation by the proteasome. Pet is the first known non-AB toxin to traffic along the retrograde pathway to the ER and then to the cytosol via ERAD (Navarro-Garcia, Canizalez-Roman et al. 2007a).

AB Toxins and ERAD

The ER provides an optimized environment for protein folding and numerous post-translational modifications such as signal peptide cleavage, N-linked glycosylation, disulfide bond formation, and the addition of a glycophosphatidylinositol (GPI)-anchors. Because there are many modifications taking place in the ER, it is important to ensure proper folding occurs. Improperly folded proteins are denied transport to other organelles of the secretory pathway. Primary quality control can detect in nascent proteins surface-exposed hydrophobic patches or reduced cysteine residues which lead to retention in the ER. The ER also retains resident proteins through the KDEL tetrapeptide motif that interacts with the KDEL receptor in a pH dependent manner (Ellgaard and Helenius 2003). The KDEL-receptor in the Golgi retrieves KDEL proteins to the ER due to the neutral pH. Some bacterial toxins such as CT possess a KDEL retrieval signal to aid in retrograde transport to the ER (Lord and Roberts 1998). Interestingly, Pet does not contain a C-terminal KDEL ER retrieval motif (Navarro-Garcia, Canizalez-Roman et al. 2007a).

ERAD is a quality control mechanism of the cell that aids in the removal of improperly folded or misassembled proteins to the cytosol for polyubiquitination and degradation by the 26S proteasome. This process is essential for the vitality of the cell because defective proteins can generate toxic aggregates or in the case of defective secretory proteins can hinder cell to cell communication. There are numerous chaperones present in the ER that bind to unfolded proteins and are capable of distinguishing an intermediate step in the folding process from a protein that will not ever assume the proper conformation and thus target it for degradation (Romisch 2005).

Pet and several AB toxins, such as CT, PT, and ricin, all traffic through a mammalian cell in the same manner and translocate from the ER to the cytosol; however they are structurally distinct (Sandvig and van Deurs 2002). AB toxins share two universal components comprised of a catalytic A subunit and a cell-binding B subunit (Hazes and Read 1997). In the ER, holotoxin disassembly occurs and the A subunit enters the cytosol where its targets resides. The holotoxin is a stable protein complex, but the A chain alone is thermally unstable at physiological temperature and unfolds. The unfolded A chain toxin is then thought to gain entry into the cytosol by triggering ERAD (Argent, Parrott et al. 2000; Pande, Moe et al. 2006; Pande, Scaglione et al. 2007).

After dissociation of the holotoxin and unfolding of the A chain, hydrophobic residues of the A chain will be exposed then recognized by chaperones in the ER. The toxin A chains are not considered typical ERAD substrates, but exploit this process to reach the cytosol then refold. Ricin and CT have been extensively studied and appear to be unfolded for retro-translocation. The refolding event that takes place in the cytosol can be mediated by the toxin's substrate which is how ricin returns to a native conformation (Roberts and Smith 2004).

Classical ERAD substrates enter the cytosol where they are polyubiquitinated on lysine residues. Ubiquitin is a tag that is recognized by the 26S proteasome, which will degrade the target protein. ERAD substrates exit the ER through the Sec61p and/or Derlin-1 channels located in the ER membrane (Bernardi, Forster et al. 2008). ER-translocating toxins escape the fate of ubiquitination and hence degradation because they contain little to no lysine residues in the catalytic A chain. For example the A subunit of PT does not have any lysine residues; CTA1 contains 2; Shiga toxin has 3; and ricin contains 2 lysine residues. The A chains of ER-translocating toxins have a codon bias for lysine and instead have arginine residues, but the B subunits of ER-translocating toxins have considerable lysine content. In comparison, the diptheria toxin A chain does not translocate from the ER and has considerable lysine content. The lack of lysine residues allow the toxin to avoid ubiquitin-dependent degradation. However, there is also degradation by the 20S proteasome, which is ubiquitin-independent. Despite the cytosolic degradation of toxin, only a small fraction is necessary to escape this fate and induce cytotoxic effects (Deeks, Cook et al. 2002; Worthington and Carbonetti 2007). In comparison, Pet does not have the structural organization of AB toxins and furthermore contains several lysine residues (Navarro-Garcia, Canizalez-Roman et al. 2007a). Therefore, we hypothesize that Pet triggers ERAD by a mechanism distinct from AB toxins.

The Structural and Folding Characteristics of the Plasmid-Encoded Toxin (Pet) from Enteroaggregative *Escherichia Coli*

The folding and export of the Pet passenger domain is thought to be a self-contained process that does not require ATP or chaperones. However, the folding efficiency of autotransporters, more specifically Pet, has not been extensively elucidated. We hypothesize that there is an inherent inefficiency in the folding process of the autotransporter Pet. Another

remaining question of the current study is how Pet, a non-AB toxin, triggers the ERAD mechanism. The A subunits of CT and ricin are thermally unstable, thus facilitating their ERAD-dependent translocation into the cytosol. However, based on its non-AB structural organization we predict that Pet does not employ thermal unfolding to exploit ERAD.

The toxin was initially purified by size exclusion chromatography in order to study the structural properties and ER export of Pet. Interestingly, Pet eluted as two peaks as confirmed through immunoblotting. The cytopathic activities of the two peaks were tested through a toxicity assay which showed that Pet peak one did not display cytotoxicity while Pet peak two did. Native gel electrophoresis, CD, and fluorescence spectroscopy were performed to rule out the possibility of Pet peak one existing as a dimer or aggregate. In addition, these biophysical measurements also differentiated the structural properties between the two peaks, and also demonstrated that Pet peak one was an unfolded variant of Pet peak two. Based on our results, our data indicates that there are two forms of Pet, and its folding process appears to be inherently inefficient.

The active, Pet peak two was used for further biophysical measurements. CD and fluorescence spectroscopy demonstrated that the secondary and tertiary structures of Pet are in a folded state at the physiological temperature of 37°C and that thermal unfolding does not occur until temperatures above 50°C. A fluorescence acrylamide quenching experiment revealed that, at 37°C, there are solvent-exposed aromatic amino acids in Pet. Furthermore, the modeled structure of Pet revealed numerous surface-exposed hydrophobic residues on a loop which connects the catalytic domain with the β-helix. This loop is of interest because it could aid the toxin in activation of ERAD. It appears that ERAD is most likely triggered through slight alterations to the structure of Pet at 37°C which produce surface-exposed hydrophobic residues.

The data therefore suggest that the mechanism in which Pet triggers ERAD is different from certain AB toxins.

CHAPTER TWO: MATERIALS AND METHODS

Circular Dichroism (CD) and Fluorescence Spectroscopy

CD and fluorescence spectroscopy of Pet was performed consecutively with the same sample using a Jasco J-810 spectropolarimeter (Jasco Corp., Tokyo, Japan). Temperature-dependent far-UV CD spectra (250-200 nm) were attained with a 0.4 cm path length quartz cuvette. The bandwidth was set to 2nm and a scanning speed set to 500 nm/min. The spectral resolution in every case was 1nm and was the average of 3 scans. Spectra were corrected by subtracting out the buffer. Concentration of the protein Pet was 45 μg /μl in 0.2 ml of 20 mM sodium phosphate (NaPi) buffer at pH 7.0. A step-wise thermal unfolding profile was obtained with temperatures ranging from 18-60°C with sample equilibration for three minutes at each temperature prior to measurement. Spectra were recorded at 2°C intervals from 18-34°C, 1°C intervals from 34-40°C, 2° intervals from 40-50°C, and 50°C, 55°C, and 60°C. The CD spectra obtained are converted from an observed ellipticity (θ_{obs}) to a mean residue molar ellipticity, [θ], with units of degrees*cm^2*$dmol^{-1}$. The per residue molar ellipticity can be obtained using the following formula: $[\theta] = \theta_{obs}/cnl$, where θ_{obs} is the calculated ellipticity in millidegrees, *c* is the molar concentration of the sample protein, n equals the number of amino acid residues in the protein, and *l* is the optical path length. Fluorescence experiments were carried out in the same manner as described for CD, except there is no correction necessary. The sample was excited at 280 nm and emission was measured between 300-400 nm. The excitation and emission slits were placed at 2 nm and 10 nm, respectively.

Temperature-Dependent Protein Unfolding

The thermal unfolding profiles were derived from CD and fluorescence spectroscopy for analysis of secondary structure and tertiary structure, respectively. For far-UV CD, the mean residue molar ellipticities at 217 nm ($[\theta]_{217}$) and 222 nm ($[\theta]_{222}$) were displayed as a function of temperature to examine the β-sheet properties and the α-helical properties of Pet, respectively. The excitation for the fluorescence measurements was 280 nm and the maximum emission wavelength (λ max) for each temperature was plotted. The analysis of the temperature-dependent protein unfolding was described using the following equation (Lavigne, Crump et al. 1998):

$$X = f_L X_L + (1-f_L) X_H \quad (1)$$

where X is the measured ellipticity at a specified temperature, f_L represents the fraction of amino acids corresponding to the native conformation at low temperatures, and X_L and X_H signify the restrictive values of X at low and high temperatures, respectively. The limits of f_L can be illustrated by

$$f_L = \exp(-\Delta G/RT)/[1 + \exp(-\Delta G/RT)] \quad (2)$$

where the free energy of unfolding (ΔG) is dependent on temperature is given by

$$\Delta G = \Delta H (1 - T/T_m) + \Delta C [T - T_m - T \ln (T/T_m)] \quad (3)$$

and ΔH symbolizes the unfolding enthalpy, T is the absolute temperature, T_m is the temperature where a transition is occurring, and ΔC can be described as the unfolding heat capacity.

Acrylamide Quenching of Pet Tryptophan Residues

The fluorescence spectra of Pet (0.45 mg/ml in 20 mM Na-phosphate buffer) was measured in a 0.4 cm path length cuvette independently at 4°C, 33°C, 37°C, 55°C, and 60°C . For each temperature Pet fluorescence spectra was taken and subsequently 1 µl of 1 M acrylamide was added to the sample. After the addition of acrylamide, the sample equilibrated for 2 minutes prior to the next fluorescence measurement. This procedure was repeated 12 times. The experiment where acrylamide was added is denoted by "F experimental," where F stands for fluorescence on the graph. For control purposes, denoted by "F control", the experiment was completed the same way with the exception of adding 1 µl of 20 mM Na-phosphate buffer each time then taking a fluorescence spectrum. The tryptophan residues of Pet were excited at 290 nm and emission was measured between 300 nm and 400 nm. The resolution of the fluorescence spectra was 1 nm. For purposes of data processing the experiment was normalized to the control to account for any variation in protein concentration. The volume (200 µl) and parameters (bandwidth) are the same for each control and experimental measurement. Normalization brought the intensities of the control spectra and the experimental spectra to the same starting point for each temperature. Determination of protein fluorescence intensity can be described by $\phi_F = k_F / \{k_F + k_{ic} + k_{is} + k_q[Q]\}$, in which ϕ_F represent the excited flurophores that emanate fluorescence with a rate constant k_F; k_{ic} corresponds to the internal conversion rate constant; k_{is} signifies the rate constant of intersystem crossing; and k_q symbolizes the rate constant of specific quenching due to a quencher at a concentration [Q]. If k_{ic} increases with increasing temperature even in the absence of apparent quenchers is thought to result in decreased protein fluorescence (Cantor and Schimmel, 1980). The quenching data were collected at a single temperature with only the concentration of acrylamide increased, so the results seen were primarily due to k_q.

Fourier Transform Infrared (FTIR) Spectroscopy

FTIR measurements were performed with a Vector 22 infrared spectrometer (Bruker Optics, Billerica, MA) installed with a liquid nitrogen-cooled Hg-Cd-Te detector, and a software-operated polarizer (aluminum grid on KRS-5 substrate, Specac, Suffolk, U.K). The resolution of the spectra was obtained at 2 cm^{-1}. Lyophilized protein from Na phosphate buffer pH 7.0 was dissolved in D_2O and directly placed between two CaF_2 windows with a 25 μm Teflon spacer. Direct transmission spectra were recorded in a temperature dependent fashion ranging from 32°C-70°C, allowing 5 minutes for equilibration between each temperature. Processing of the spectra was done using Grams/AI (7.01) software (ThermoGalactic, Salem, NH). The spectra were corrected for evaluation of the secondary structure, and components of amide I (1700-1600 cm^{-1}) were obtained using curve-fitting. The curve-fitting was based on the quantity and location of peaks from the second derivative inverse spectra. Curve-fitting results were deemed acceptable when all the component frequencies were within a ±1 cm^{-1} range in comparison to the input frequencies. Also, the sum of all the components was concurrent to the calculated spectrum and this also determines further validity.

Protease Sensitivity Assay

A master mix for each protein was prepared with 6 μg of each protein containing 10 mM β-ME, 20 mM Na-phosphate buffer (pH 7.0), and sterile water to 120 μl final volume. Five tubes were then labeled "pure," 4°C, 25°C, 33°C, 37°C, 41°C and 20 μl aliquots of the master mix were placed in each tube. The samples were then incubated at the appropriate temperatures for 1 hour with the "pure" tube placed at 4°C. After the 1 hour incubation the samples were placed on ice at 4°C for 10 minutes. Thermolysin, at a concentration of 0.4 mg/ml, was subsequently

added and incubated for another hour at 4°C. The samples contained a final concentration of thermolysin of 0.006 mg/ml. Sterile water was added to the "pure" tube. After protease treatment 100 mM ethylenediaminetetraacetic acid (EDTA) and sample buffer were combined with the samples and sterile water was placed in the "pure" tubes. Samples were boiled and visualized by sodium dodecyl sulfate- polyacrylamide gel electrophoresis (SDS-PAGE) and Coomassie staining. CTA1 subunit was processed as described above for Pet and used for a control. In addition, two separate experiments were performed with the two mentioned toxins in the presence of equimolar fodrin (Canizalez-Roman and Navarro-Garcia 2003).

Pet Immunoblot

The concentration of Pet was 0.5 mg/ml and 500 ng was loaded on an 8% SDS-PAGE gel. After performing electrophoresis for 1 hour and 15 minutes at 150 volts the acrylamide gel was equilibrated for 20 minutes in transfer buffer, which consists of 1X running buffer, pure methanol, and water. Bio-Rad Protean ® XL size extra thick blot paper was also soaked in transfer buffer for 10 minutes. The polyvinylidene fluoride (PVDF) membrane was soaked in 100% Methanol for 1 minute the placed in transfer buffer for 1 minute. For the transfer a gel sandwich was prepared on the transfer apparatus in the following order: pre-wet filter paper, pre-wet membrane, equilibrated gel, and the other pre-wet filter paper. The gel sandwich is rolled out to release any bubbles between the layers. The transfer was run at 10 volts for 20 minutes and the increased to 15 volts for 40 minutes. After the transfer was complete the membrane was placed in a plastic square dish with Tris-buffered saline-Tween 20 (TBS-T) and India ink for about 15-20 minutes at room temperature. The India ink allowed for visualization of the protein bands. After staining with India ink the membrane was rinsed twice with TBS-T 2 times for 5 minutes.

All of the liquid was poured off and TBS-T with 5% skim milk was added to the plastic square dish, rocked for about 10 minutes at room temperature, covered with parafilm, and placed at 4°C overnight. The next morning the membrane was washed with 1% TBS-T milk twice for 10 minutes each. The surf blot for adding primary antibody (Ab) was prepared. The membrane was placed protein side down on the surf blot, ensuring that the protein band strattles the lane, then a piece of parafilm was placed over the membrane. On top of the parafilm a sponge was placed followed by a steel plate which was sealed by 2 large binder clips to each side. Flipping over the surf blot apparatus the primary Ab was added to the corresponding protein lanes. The primary Ab used was rabbit anti-Pet used at a 1:300 dilution (Eslava, Navarro-Garcia et al. 1998). The primary Ab was incubated on the rocker at room temperature for 1 hour. After incubation the Ab was removed from the surf blot and the membrane was placed in a plastic square dish and washed three times for 10 minutes each with 1% TBS-T milk. After the three washes the secondary Ab (goat anti-rabbit-peroxidase-conjugated IgG) at a 1:20,000 dilution was added and incubated for 1 hour at room temperature. After the secondary incubation the 1% TBS-T milk plus secondary Ab was poured off and the membrane was rinsed three times with just TBS-T for 10 minutes each. While the membrane was rinsing the working solution of Pierce Supersignal Enhanced Chemiluminescence (ECL) reagent was prepared by mixing a 40:1 of A: B dilution. After the three washes the working solution was poured on the protein side of membrane and incubated for 5 minutes. The ECL solution was drained after the incubation and placed on the developing cassette. The cassette was immediately taken to the dark room for exposure on film.

Toxin Preparation and Purification

The experiments performed were carried out with lyophilized Pet protein sent as a gift from Dr. Navarro-Garcia, resuspended in ddH_2O, filtered, and purified as previously described (Navarro-Garcia, Canizalez-Roman et al. 2007a). Pet was expressed from *E. coli* HB101, a nonpathogenic lab strain transformed with the pCEFN1 Pet expression vector. The cultures were grown overnight at 37 °C in 100 ml of Luria-Bertani broth (LB broth) in the presence of ampicillin at a concentration of 100 μg/ml to obtain the Pet protein. Once the bacteria reached an optical density (OD_{600}) of 0.6-0.8, which corresponds to the late logarithmic phase, they were subjected to centrifugation at 12,000 X g for 10 minutes. (Navarro-Garcia, Canizalez-Roman et al. 2001). After centrifugation the supernatant was filtered through a 0.22-μm cellulose acetate membrane filter (Corning, Cambridge, Mass), and was concentrated with 50 kDa ultrafiltration spin columns (Vivaspin 20; Sartorius Biolab, Goetingen, Germany). For the purpose of removing the LB broth, the sample was filter sterilized through a 2 μM syringe filter and loaded onto a HiLoad 16/60 Superdex 75 size exclusion column (Amersham) using an ÄKTA purifier (GE Healthcare). The pure Pet protein was collected in 1 ml fractions at a rate of 0.5 milliliter per minute in elution buffer (20 mM Tris pH 7.4 and 25 mM KCl). This produced two peaks and the fraction samples were collected, concentrated with a 30,000 molecular weight cut-off filters (Millipore, Bedford, MA), dialyzed at 4 °C against 20 mM Na-phosphate buffer at pH 7.0, and immediately used for biophysical measurements.

Computational Modeling of SPATES

The structure of Pet was modeled using hemoglobin protease, a SPATE that has been crystallized (PBD_1WXR) (Otto, Sijbrandi et al. 2005). The model of Pet was generated with

the ESyPred3D online structure predictor (Lambert, Leonard et al. 2002) located at the ExPASy website (http://www.fundp.ac.be/urbm/bioinfo/esypred/). Pet and hemoglobin protease share 28.2% sequence identity and 43% sequence homology with respect to their passenger domains. In addition, four other SPATE proteins, EspP, EspC, SepA and SAT (secreted autotransporter of uropathogenic *E. coli*) were modeled using hemoglobin protease as a template. The models, space filling and ribbon diagrams, were created with the WebLab Viewer Lite program.

Pet Denaturation and Renaturation

After size exclusion chromatography, Pet peak one or two was denatured in 4 M guanidine hydrochloride (HCl) and 20 mM Dithiothreitol (DTT) using elution buffer (150 mM KCl and 25 mM Tris-base, pH 7.4) as the solvent. The concentration of Pet was 200 μg/ml and 1.5 mls was used in the experiment. Denaturation was carried out at room temperature by gently agitating the sample in a 15 ml conical overnight. Renaturation was achieved through a step-wise decrease in guanidine hydrochloride (HCl) and DTT. The first step of renaturation was transferring the sample to a Slide-A-Lyzer® 20,000 molecular weight cut off dialysis cassette (Thermo Scientific, Rockford, IL). Subsequently, the dialysis cassette was placed in 0.5 L of buffer with 2 M guanidine HCl and 5 mM DTT. Dialysis at 2M guanidine HCl proceeded for 2 hours at room temperature with stirring. Following 2 M dialysis, 1M guanidine HCl and 2.5 mM DTT continued overnight as previously described. Next, 0.5M guanidine HCl and 1.5 mM DTT, 0.1 M guanidine HCl and 0.5 mM DTT were carried out for two hours each, and finally the sample was subjected only to elution buffer. The renatured Pet protein was placed on the size exclusion column as previously stated and collected in 0.5 ml fractions. CD and fluorescence spectroscopy of the peak fractions were collected.

Cell Rounding Pet Toxicity Assay

Pet peaks one and two (40 μg/ml) were added to separate samples of CHO cells seeded in a 24-well plate for a total volume of 250 μl containing Ham's F-12 medium enhanced with 10% fetal bovine serum and penicillin/streptomycin. Toxin-free medium was added to a well for control purposes. The cells were incubated at 37 °C for 24 hours and pictures were taken with a digital camera with 10X magnification mounted on a Zeiss (Gottingen, Germany) Axiovert 25 microscope (Navarro-Garcia, Canizalez-Roman et al. 2007a).

CHAPTER THREE: RESULTS

Project #1: The Folding Characteristics of Pet: Purification of Pet

Autotransporter secretion is not well characterized, but it is thought to be energy-independent due to the lack of significant ATP concentration in the periplasm, and a proton gradient does not exist across the outer membrane (Renn and Clark 2008). Folding and secretion of autotransporters is considered a self-contained process, where all the domains necessary for secretion are encoded within the proprotein. In this section we looted the hypothesis that autotransporter folding is an efficient, autonomous process.

Pet was expressed and lyophilized as formerly described in the Methods section. After the expression of Pet, native gel electrophoresis was performed and revealed a single band at 104 kDa corresponding to the molecular mass of Pet (Figure 1A). The single band from native gel electrophoresis suggests that Pet was not isolated as a dimer or aggregate; otherwise higher molecular mass protein bands would have been detected. In addition, the stacking portion of the gel was also stained and did not show the presence of protein (data not shown). Further purification of Pet was necessary because the mature protein was expressed and lyophilized in LB broth which would interfere with the signal obtained from biophysical measurements such as CD and fluorescence spectroscopy. Lyophilized Pet was resuspended in ddH_2O and filter sterilized just prior to loading onto the hi-load 16/60 75 Superdex size-exclusion column. Pet fractionation produced two peaks that were consistently observed to elute at ~ 42 mls and ~ 48 mls corresponding to Pet peaks one and two, respectively (Figure 1B). Based on the elution profile of the fractionation it appears that Pet peak one is present at a higher concentration than Pet peak two. Both peaks were confirmed Pet through immunoblotting (Figure 1C). However,

Pet peak one over time generates degradation products which suggests its instability. Interestingly, if after fractionation the samples are not immediately placed in sample buffer then degradation products are seen on the immunoblot. There is also a possibility that these degradation products are due to autoproteolysis or even trace contaminating proteases.

In order to determine the differences in functionality between the two peaks of Pet, a toxicity assay was performed and each peak was added separately to CHO cells at 40 μg toxin/ml. The results demonstrated that Pet peak one did not display cytopathic effects while intoxication with peak two resulted in cell rounding and detachment from the substratum (Figure 2). We thus isolated two 104 kDa variant forms of Pet that differed in the elution profile, stability, and toxicity.

Earlier elution of Pet peak one may be due to an unfolded or open conformation, consistent with toxicity data. To ensure that the elution buffer did not induce a portion of Pet to assume an unfolded conformation, Pet peak two was repurified (Figure 3). The elution profile of the repurification reveals one peak at ~ 54 mls (Figure 3A). CD spectroscopy was performed on the sample to verify the structure of the peak (Figure 3B). The CD spectra showed a minima at 214 nm, indicating that this peak has considerable β-sheet structure. This is consistent with the CD spectra of Pet peak two from the initial purification. As a result, the two Pet variants are not due to the buffer or the chromatography process itself.

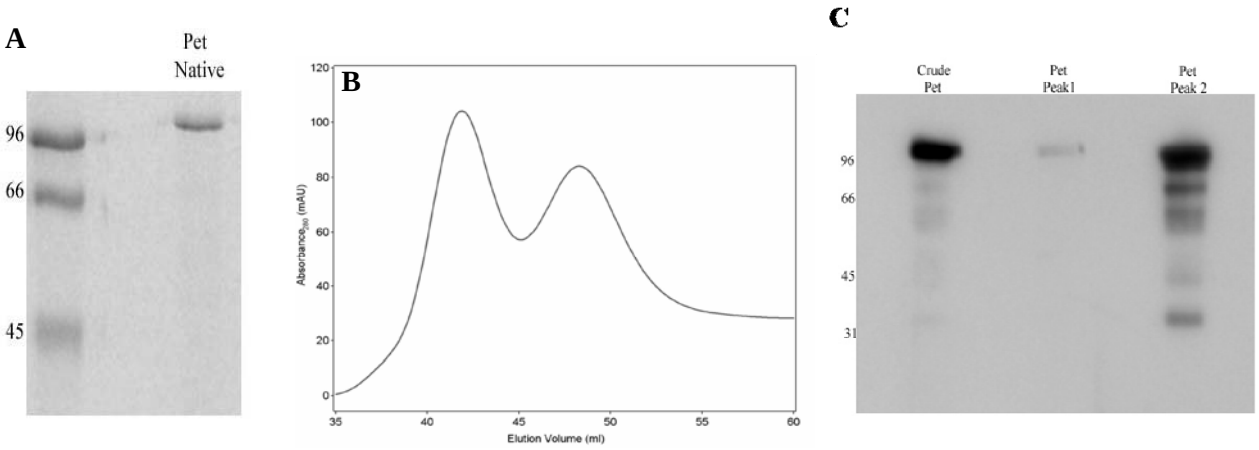

Figure 1: Pet Purification Produces Two Peaks

(A) Native gel electrophoresis of Pet prior to size exclusion chromatography. Molecular mass of protein standards (left most lane) are indicated. (B) Size exclusion elution profile of fractionated Pet. Pet peak one elutes at ~ 42 mls and Pet peak two elutes at ~ 48 mls. (C) Both peaks were confirmed Pet through immunoblotting with a rabbit α-Pet polyclonal antibody. Crude Pet indicates pre-chromatography toxin.

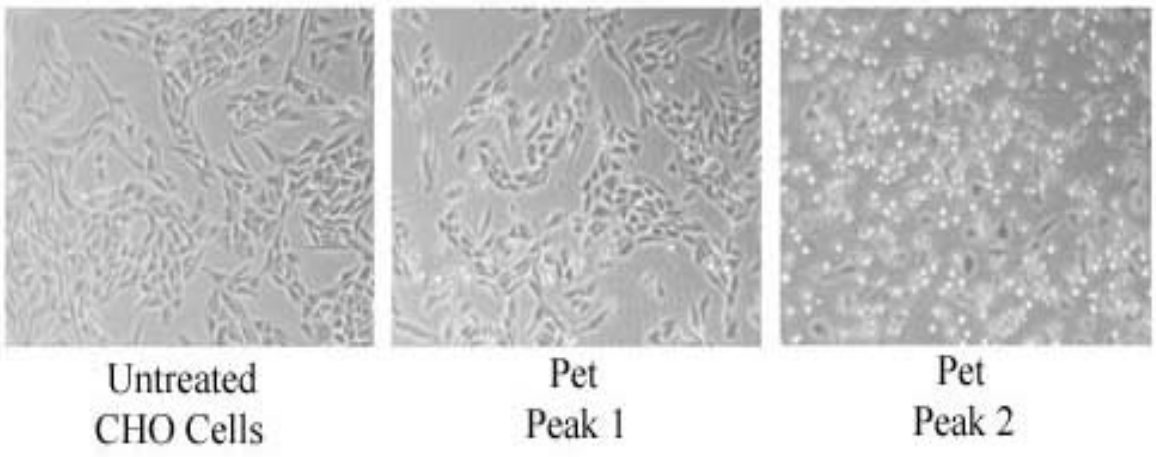

Figure 2: Pet Peaks One and Two Toxicity Assay

Either toxin-free media or Pet-containing media at a concentration of 40 μg/ml was added to CHO cells and incubated overnight at 37°C. Phase contrast images at 10X magnification with a digital camera mounted on a Zeiss (Gottingen, Germany) Axiovert 25 microscope.

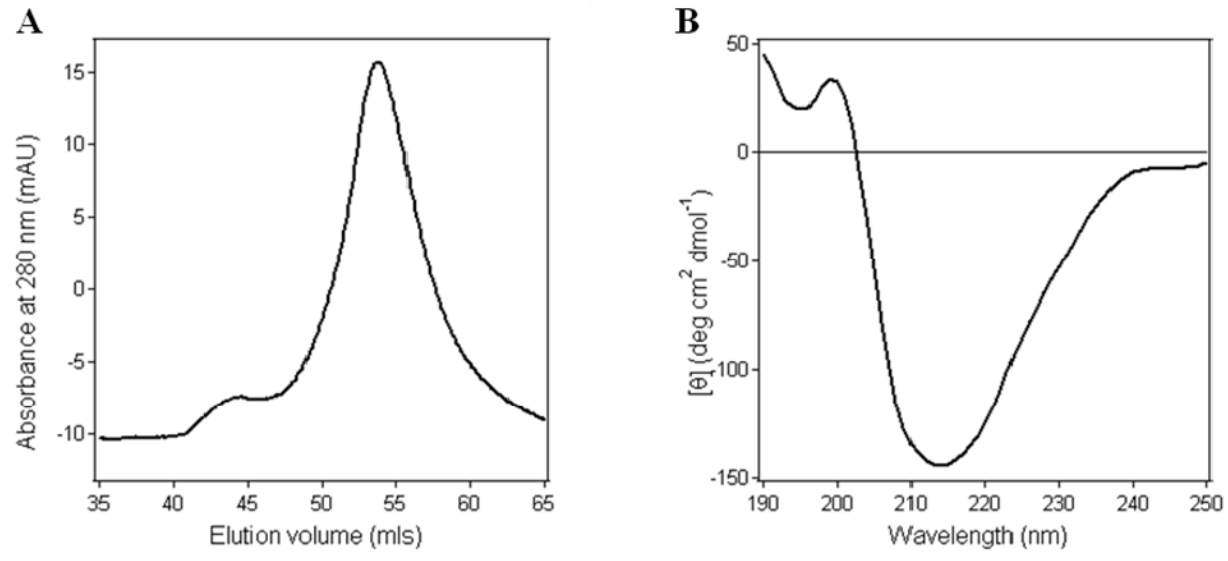

Figure 3: Non-Induced Buffer Unfolding of Pet

(A) Size exclusion elution profile of refractionated Pet peak two. The peak eluted at ~ 54 mls.
(B) Far-UV CD spectra of the peak in panel A measured at 18°C in a 0.4 cm path length cuvette. Far-UV CD spectra represent the secondary structure of Pet peak two.

Structural Properties of Pet Peak One

Far-UV CD and fluorescence spectroscopy were performed to determine the structural properties of Pet peaks one and two. The buffer was exchanged to 20 mM NaPi just prior to the biophysical measurements. The concentration of Pet peak one was 0.31 mg/ml, and the concentration of Pet peak two was 0.45 mg/ml. The differences between the secondary and tertiary structures of the two peaks were considerably different (Figure 4). Pet peak one contains unordered secondary structure with a single minimum at 207 nm and a maximum at about 200 nm at temperatures including 37°C. In comparison, Pet peak two contains significant β-sheet secondary structure with a single minimum at 217 nm and a maximum at about 200 nm (Figure 4A and 5A). The tertiary structures, as shown by fluorescence spectroscopy, of Pet peaks one and two can be distinguished by the λ_{max} values (Figure 4B). At 18°C the λ_{max} of Pet peak two was 327 nm, while the λ_{max} of Pet peak one was significantly shifted to 342 nm. The maximum emission wavelength (λ_{max}) of Pet peak one fluorescence is about 342 nm and a red shift was also observed at about 56°C. The observed red shift compared to peak two implies that Pet peak one does not exist as a dimer or aggregate of Pet peak two, and this data is also consistent with the native gel shown in figure 1A. If Pet peak one did exist as a dimer or aggregate then a blue shift would be detected, and the λ_{max} shifts to a lower wavelength. A blue shift would indicate that the aromatic amino acid residues are not solvent-exposed. Further characterization of Pet peak two was performed in project #2.

Project #1 examines the structural properties of Pet peak one and the comparison of the two peaks. The temperature-dependent far-UV CD measurements were taken in a step-wise manner increasing in temperature from 18°C to 60°C (Figure 5). The tertiary structure of Pet peak one was examined by fluorescence spectroscopy and the spectrum were collected in step-

wise increments from 18°C to 60°C (Figure 5B). Pet peak one tryptophan, tyrosine, and phenylalanine residues were excited at 280 nm. The maximum emission wavelength (λ_{max}) of Pet peak one fluorescence is about 342 nm and a red shift was also observed at about 56°C. These results suggest that Pet peak one is initially in a more open conformation with the tryptophan residues solvent-exposed. This apparent unstable open conformation most likely accounts for why Pet peak one elutes first during size exclusion chromatography. In addition, the inactivity of Pet peak one indicates that the toxin is not in a native conformation. The results suggest that Pet peak one is an unfolded variant of the active Pet peak two.

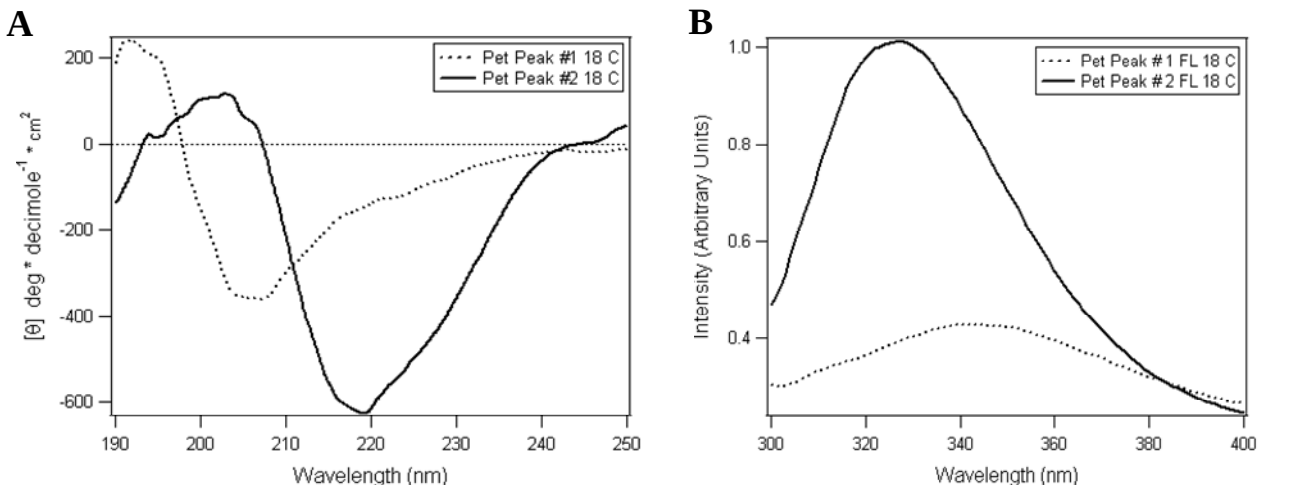

Figure 4: Comparison of Pet Peaks One and Two

(A) Far-UV CD spectra of Pet peaks one (dashed line) and two (solid line) at 18°C are shown. (B) Fluorescence spectra of Pet peaks one (dashed line) and two (solid line) at 18°C. Measurements by far-UV CD and fluorescence spectroscopy were performed on the same sample, where Pet peak one was at concentration of 0.31 mg/ml and Pet peak two was at a concentration of 0.45 mg/ml.

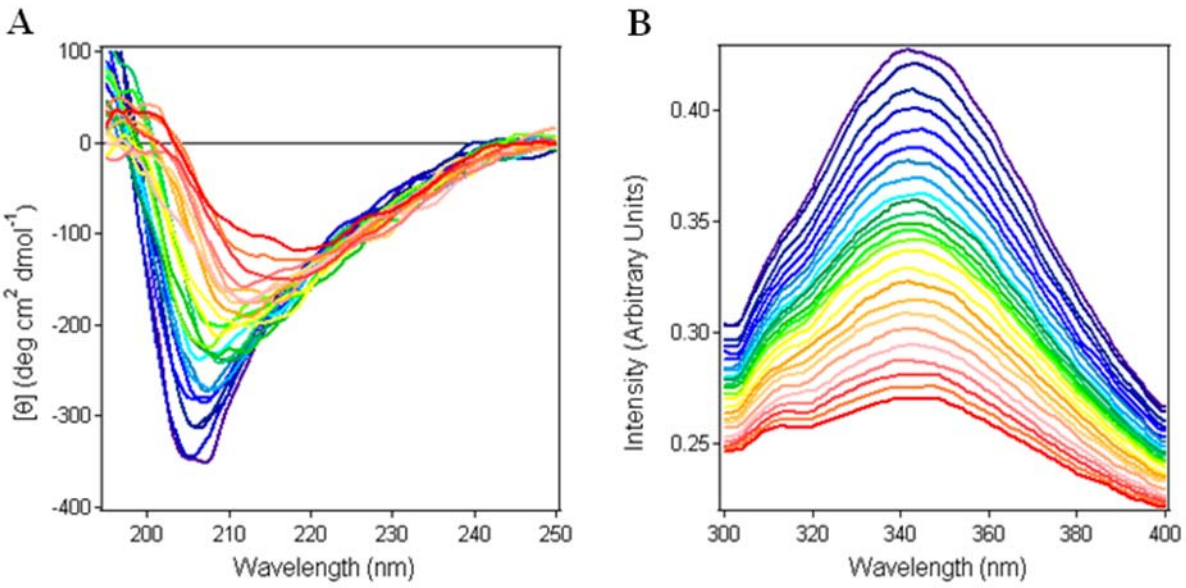

Figure 5: Far-UV CD and Fluorescence Spectroscopy Measurements of Pet Peak One

(A) The far-UV CD spectra of Pet peak one were measured during a step-wise increase in temperatures from 18°-60°C. The far-UV CD spectra represents the secondary structure of Pet peak one. (B) Fluorescence spectra of Pet peak one measured during a step-wise increase in temperature from 18-60°C. For both panels, the change in color from purple to red indicates the change in temperature from 18°C to 60°C.

The Folding Characteristics of Pet Peaks One and Two

A substantial pool of Pet secreted from HB101 is in an unfolded conformation. The folding of autotransporters is thought to be a self-contained, energy-independent process that does not require the assistance of chaperones (Renn and Clark 2008). To further examine the folding efficiency of the autotransporter Pet, both peak one and peak two were independently denatured in 4 M guanidine hydrochloride and 20 mM Dithiothreitol (DTT) overnight at room temperature. After denaturation the sample was dialyzed in a step-wise manner at room temperature with decreasing concentrations of guanidine hydrochloride and DTT until Pet was only in size exclusion buffer (150 mM KCl and 25 mM Tris pH 7.4). After denaturation and renaturation the Pet samples were loaded onto the size exclusion column and recovered for biophysical analysis (Figure 6). If the folding and export of autotransporters is a self-sufficient process, then one would expect to see a portion of Pet peak one regain a native conformation after it has been denatured and renatured.

The elution profile after renaturation of Pet peak one demonstrates only one peak that elutes at the same volume as the original peak one (Figure 6A). With the exception of concentration differences between Pet peak one samples before and after denaturation and renaturation, the far-UV CD spectra of both samples exhibited about the same maxima and minima (Figure 6B). Based on the result of this experiment the unfolding event appears to be irreversible, and once Pet peak one is unfolded it will not achieve an active conformation.

The denaturation and renaturation of Pet peak two produced two peaks, and both fractions were at the same elution volume as the initial purification fractionation (Figure 6C). Figure 6D presents the far-UV CD measurements for the Pet peak two experiment, and shows three spectra: (i) Pet peak two after the initial fractionation purification (solid line); (ii) peak one from the

denaturation/renaturation peak two fractionation (dotted line); (iii) peak two from the denaturation/renaturation peak two fractionation (open circles). The appearance of peak one after the denaturation/renaturation of Pet peak two signifies that the original peak one is not an artifact of the initial purification procedure in Dr. Navarro-Garcia's protocol. The possibility of Pet peak one arising from an erroneous post-translational modification is not likely, since we obtained peak one from a pool of toxin (peak 2) that represented 100% properly folded toxin. In addition, to demonstrate that the size exclusion buffer was not altering the folding of the Pet, peak two was immediately repurified. In this experiment, peak one was not present. Thus, the appearance of peak1 in the denaturation/renaturation experiment is not simply due to running the material over the column. We started with a folded pool of toxin, and after denaturation/renaturation only a portion of it was properly (re)folded. The current autotransporter model predicts autonomous refolding, so the denaturation/renaturation experiment should just produce peak 2. Collectively, these experiments provide evidence for an inefficient folding event of the autotransporter Pet.

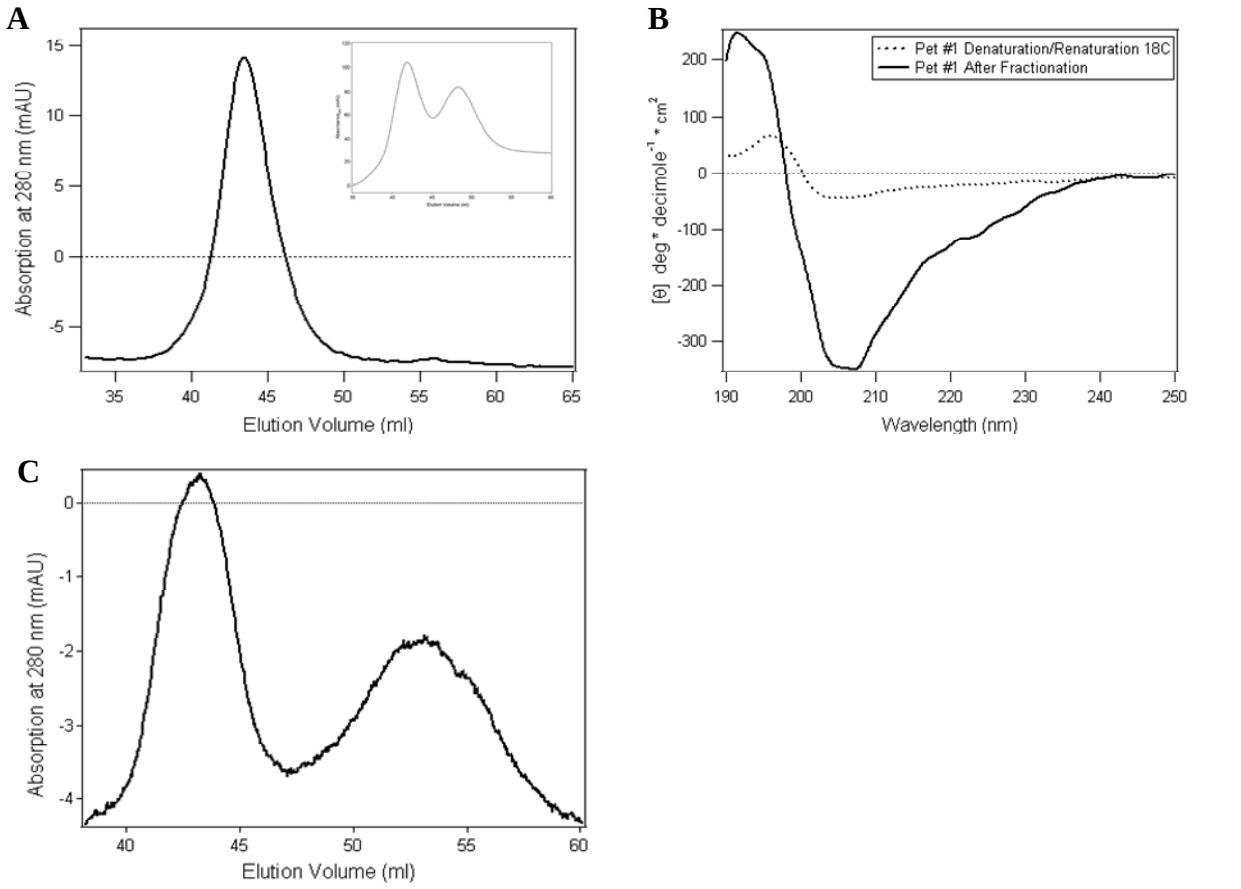

Figure 6: Denaturation and Renaturation of Pet Peaks One and Two Followed by Size Exclusion Chromatography

Pet peaks one and two were denatured overnight at room temperature with 4M guanidine hydrochloride and 20 mM DTT. After denaturation the sample was dialyzed in a stepwise manner at room temperature with decreasing concentrations of guanidine hydrochloride and DTT until Pet was only in size exclusion buffer (150 mM KCl and 25 mM Tris pH 7.4). After denaturation and renaturation the Pet samples were loaded onto the size exclusion column. Panels A and C represent the chromatograms of the Pet peak one and two, respectively, after denaturation/renaturation. The inset in panel A represents the initial fractionation elution profile of Pet. Far-UV CD in panels B and D were performed on Pet peaks one and two before (solid line) and after (dotted line) denaturation/renaturation.

Pet Expressed from EAEC

Since Pet was purified from the HB101 lab strain of *E. coli*, it was possible that the efficient folding of Pet required a chaperone or other factor which is only present in the pathogenic strain of enteroaggregative *E. coli*. To identify possible differences between Pet produced in HB101 vs. EAEC, the toxin was purified from an EAEC strain of *E. coli* and purified by size exclusion chromatography (Figure 7). Only one peak was detected as shown by the elution profile and confirmed Pet through immunoblotting (Figure 7A and B). However, other bands with a molecular weight less than 104 kDa are observed and there is a possibility that these are degradation products due to autoproteolysis or even trace contaminating proteases. Far-UV CD analysis was performed on the peak fraction and the spectra revealed a minimum at about 213 nm (Figure 7C). Our data indicate that the variant expressed by an EAEC strain of *E. coli* is the same as Pet peak 2 produced by HB101.

The vast majority of the toxin produced in HB101 is not in a native conformation and inactive (Figure 1B, 2). The elution profiles of Pet purified from HB101 vs. an EAEC strain of *E. coli* show that folding is optimal when expressed from a pathogenic strain of *E. coli*. Furthermore, this suggests that a pathogen-specific factor is necessary for efficient folding of the autotransporter Pet. Interestingly, autotransporter folding is thought to be a self-contained autonomous process without the assistance of chaperones.

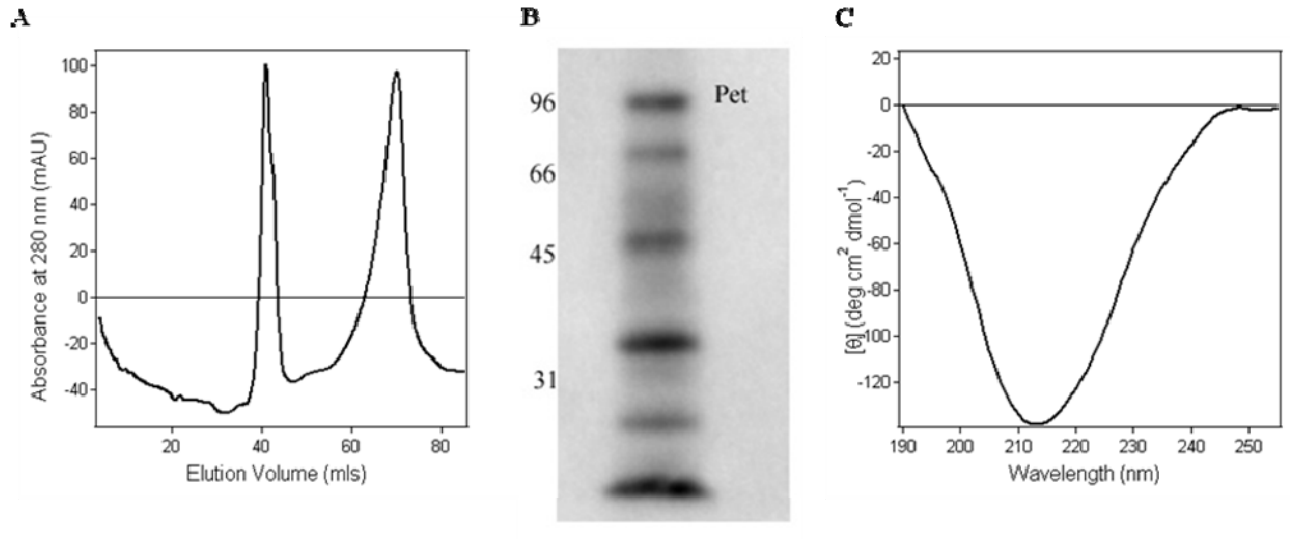

Figure 7: Size Exclusion Chromatography of Pet Purified from an EAEC Strain of *E. coli*

(A) Size exclusion elution profile of fractionated Pet from an EAEC strain of *E. coli*. The first peak eluted at ~42 mls and the second peak at ~70 mls. (B) The first peak was confirmed Pet through immunoblotting with a rabbit α-Pet polyclonal antibody. (C) Far-UV CD was performed on the first peak at 18°C in a 0.4 cm path length cuvette. Far-UV CD spectra represent the secondary structure of that is similar to Pet peak two purified from a lab strain of *E. coli*.

Project #2 Conformational Stability of Pet: Structural Properties of Pet

Project #1 showed that there are two variants of Pet, peaks one and two. Peak two was the functional cytopathic variant, while peak one was an unfolded inactive variant. Therefore, all studies in this section were performed with active Pet peak two. In order to determine the mechanism by which Pet triggers ERAD, the structural properties and thermal stability of Pet are determined by far-UV CD and fluorescence spectroscopy. The A subunits of certain toxins such as CT and ricin are thermally unstable, and this facilitates their ERAD-dependent translocation into the cytosol. Pet, however, is not an AB toxin, and is structurally distinct from the A chains of AB toxins. We therefore predicted that Pet triggers ERAD activity by a different mechanism than the AB toxins. This was tested by establishing the conformational stability of Pet.

Prior to the biophysical measurements the buffer was exchanged to 20 mM NaPi, and Pet was used at a concentration of 0.45 mg/ml. Measurements were taken in a step-wise manner increasing in temperature from 18°C to 60°C (Figure 8). The data clearly depicts a single minimum at 217 nm at lower temperatures, indicating that Pet's mature chain contains significant β-sheet secondary structure (Figure 8A). As the temperature increased to 52°C a steady loss of Pet secondary structure was observed, and at temperatures above 52°C the loss of structure was more pronounced (Figure 8B). This two step transition of unfolding was also reported by Renn and Clark (2008), but in their study a chemical denaturant was employed instead of temperature. After reaching 60°C, the sample was cooled in a step-wise fashion back to 18°C (Figure 8B, open circles). The measurements taken during sample cooling demonstrate that the loss of structure due to heating was irreversible. At physiological temperature, Pet merely lost 23% of its secondary structure when compared to the initial spectra taken at 18°C. The loss of Pet secondary structure at 37°C is considerably less than other ER-translocating

toxins: the enzymatic A subunits of CT and PT lose 44% and 88% of their secondary structures, respectively at 37°C (Pande, Moe et al. 2006; Pande, Scaglione et al. 2007).

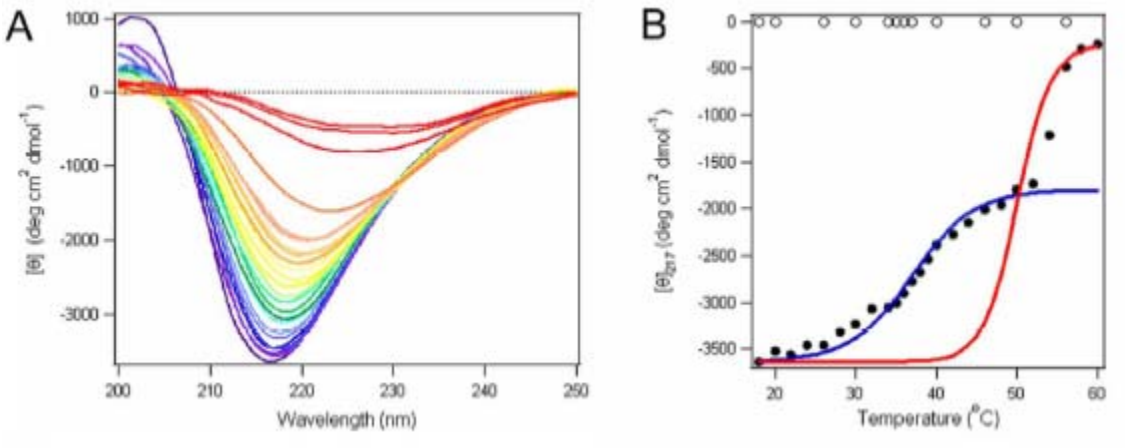

Figure 8: Thermal Stability of Pet Secondary Structure

(A) The far-UV CD spectra of Pet (0.31 mg/ml in 20 mM NaPi) were measured in a 0.4 cm path length cuvette during a step-wise increase in temperature from 18°-60°C as indicated by the color change from purple to red. (B) The change in $[\theta]_{217}$ is plotted as a function of temperature to monitor variations in secondary structure (filled circles). Also shown is Pet refolding during sample cooling from 60°C to 18°C at $[\theta]_{217}$ (open circles). The blue and red lines represent simulated curves. For first and second transitions, respectively.

The thermal stability of Pet's tertiary structure was examined by fluorescence spectroscopy. The experiment was carried out with 0.45 mg/ml of purified Pet in NaPi buffer, and spectra were collected from 18°C to 60°C in a step-wise increase. Pet tryptophan, tyrosine, and phenylalanine resides were excited at 280 nm. The seven tryptophan residues in the mature chain of Pet represent the observed emission wavelengths of 326-333 nm (Figure 9A). Fluorescence intensity is dependent upon temperature, therefore with increasing temperature there is a decrease in the signal, but has no bearing on protein conformation (Cantor and Schimmel 1980). This phenomenon is observed from 18°C to 40°C (Figure 9A, inset). Fluorescence intensity decreased more rapidly above 40°C indicating a change in protein conformation and a T_m value of 46°C. In fluorescence spectroscopy a red shift occurs when the maximum emission wavelength (λ_{max}) progresses to a larger λ_{max}, this signifies solvent exposure of tryptophan residues and, ultimately, a change in protein compaction. A red shift to Pet λ_{max} occurred when the temperature surpassed 40°C. The thermal unfolding profile of Pet demonstrated a T_m value of 50°C (Figure 9B). For both fluorescence intensity and $\lambda_{max,}$ there are negligible differences between the initial low temperature measurements and the 37°C measurements. This indicated that there was minimal solvent exposure of Pet tryptophan residues at 37°C.

Near- UV CD was also performed as another method of examining the tertiary structure of Pet in a temperature dependent system (Figure 9C-D). More specifically, near UV-CD (250-350nm) is sensitive to the side chains of aromatic residues including phenylalanine, tyrosine, and to a greater extent tryptophan. This method detects the subtle changes in conformation of the tertiary structure of a protein (Permyakov, Bakunts et al. 2008). Pet near-UV CD revealed several components, two stronger bands at 270 nm, 280-288 nm and a weaker component around

250-260 nm (Figure 9C). Components generated in 250 nm range correspond to the π-π^* transitions of the aromatic residues phenylalanine and tyrosine and also by the n-σ^* disulfide bond transitions. Tyrosine and tryptophan residues also contribute in this area but produce a stronger signal around 280-290 nm (Sreerama and Woody, 2000; Woody and Dunker, 1996). The near-UV CD signals are significantly due to the seven tryptophan and twenty-nine tyrosine residues since Pet only contains two cysteine residues that most likely do not form a disulfide bond. The near-UV CD data displayed a biphasic temperature dependence at all three components; 250, 270, and 280 nm. As the temperature increased from 18°C to 40-45°C there was a gradual increase in signal intensities from negative values to more positive values and at higher temperatures the signal decreased again (Figure 9D). All three components exhibited the same trend: from 18°C to 40-45°C Pet became more unstable or assumed an open conformation, and at temperatures above 45°C the protein became aggregated which would cause the spectra to appear as though the tertiary structure was more compact.

The difference between the near- and far-UV CD indicate that thermal destabilization occurs more quickly in the tertiary structure as opposed to the secondary structure when Pet is heated from 18°C to 40-45°C. In contrast, the fluorescence data suggest that tryptophan exposure to solvent does not occur until temperatures above 40°C. There are differences because near-UV is more sensitive, it picks up changes not detected by fluorescence spectroscopy. However, more dramatic structural changes occur only at temperatures at or above 40°C (λ_{max}). This result was consistent with the thermal profile for the secondary structure of Pet. All three measurements (far-UV, fluorescence spectroscopy, and near-UV) demonstrated that significant thermal destabilization of Pet only occurred at temperatures above 50°C. Collectively, the data indicate that the tertiary and secondary structures of Pet undergo minor thermal alterations at

physiological temperature. Substantial unfolding of the toxin only occurs at high temperatures. This is drastically different from the typical AB toxins that translocate from the ER, such as CT and PT, because at 37°C the toxin A chains are in an unfolded state (Pande, Moe et al. 2006; Pande, Scaglione et al. 2007).

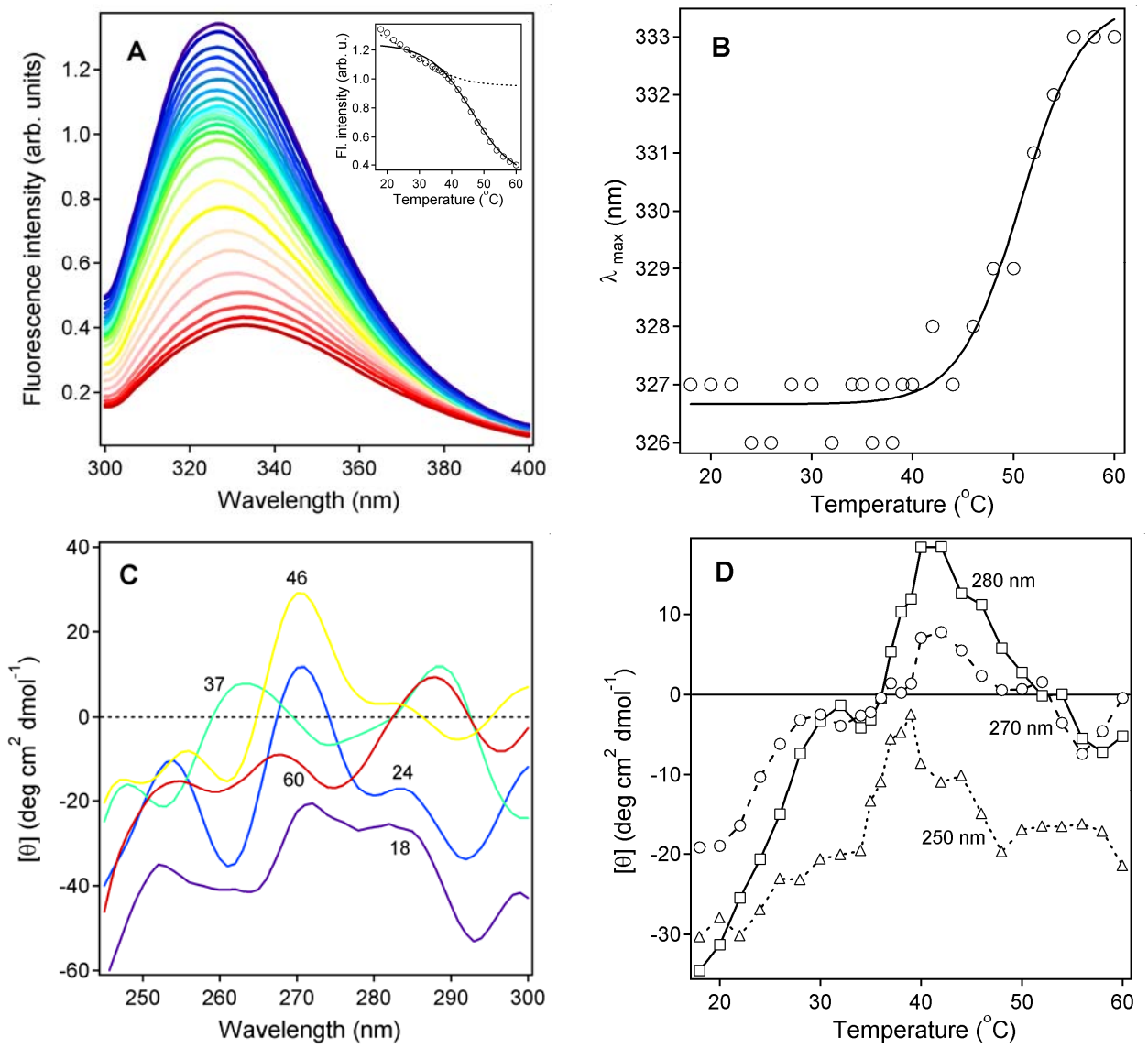

Figure 9: Thermal Stability of Pet Tertiary Structure

(A) Fluorescence spectra of Pet measured during a step-wise increase in temperature from 18-60°C, as shown by the change in color from purple to red. The inset of panel A represents the temperature dependence of fluorescence intensity. The dashed line signifies the first transition which is the intrinsic temperature dependence of fluorescence intensity. The second transition, displayed as a solid line, corresponds to the conformation dependence of fluorescence intensity. (B) The λ_{max} of Pet fluorescence is derived from the data in panel A, and is plotted as a function of temperature. (C) Spectra of Pet near-UV CD measured during a stepwise increase in temperature from 18°C to 60°C. Select spectra of Pet, indicated by the labeled temperatures on the graph (18°C, 24°C, 37°C, 46°C, and 60°C), are shown for simplicity. The colors match the temperatures of other CD and fluorescence data. (D) Alterations to three components (250, 270, and 280 nm) of the near-UV CD spectra (panel C) are presented as a function of temperature.

Refolding of Pet Tertiary Structure

One way a toxin may elicit the ERAD response is by a thermal ratchet mechanism employed by ricin A chain. The thermal ratchet mechanism utilizes thermal fluctuations to create slight irreversible alterations in the toxin structure (Argent, Parrott et al. 2000). These changes ultimately generate a protein that is unfolded, but at temperatures that would not usually affect the conformation of the toxin. To further elucidate Pet's mechanism of ERAD activation and determine if there is a possibility that Pet exploits ERAD in the same manner as ricin, a refolding experiment using fluorescence spectroscopy was performed (Figure 10). First, a reference spectra was recorded for purified Pet heated to 37°C in a step-wise manner. The next sample was heated to 41°C in the same way, cooled in a step-wise decrease back to 37°C, and then a fluorescence spectra was taken. This was repeated for three other temperatures that reached 45°C, 50°C, and 60°C. A separate toxin sample was used for each temperature. It can be seen that the fluorescence maximum emission wavelength was not significantly affected even after heating to 45°C and cooling back to 37°C. However, at temperatures above 45°C a red shift in λ_{max} was generated when the sample of Pet was cooled back to 37°C. It is evident from this experiment that at 50°C and 60°C the unfolding event was irreversible. Given that the irreversible loss of tertiary structure involves temperatures above 45°C, the thermal ratchet mechanism employed by ricin is not a probable way Pet triggers ERAD at near physiological temperatures.

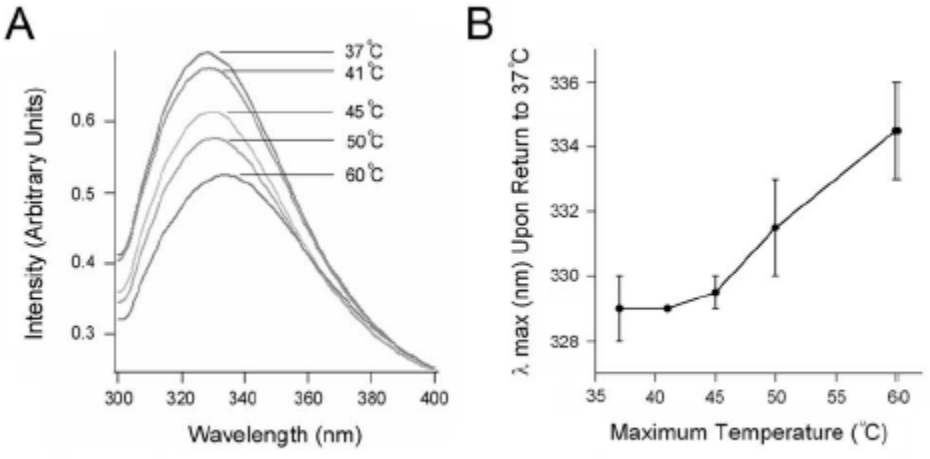

Figure 10: Refolding of Pet Tertiary Structure

The fluorescence spectra were measured after each sample was cooled from the specified temperature to 37°C. A different sample was used for each experiment. The experiment was performed twice and one of two experiments is shown in (A); in (B) the average of λ_{max} from both experiments is plotted.

The Hydrophobic Properties of Pet

The tertiary structure of Pet was monitored in a temperature dependent fashion in Figure 9, but its surface hydrophobicity was not determined. The hydrophobic properties of Pet can be examined through fluorescence quenching (Cantor and Schimmel, 1980). Surface-exposed hydrophobic residues of Pet in its native conformation could be the trigger to activate ERAD; this could occur without considerable structural alterations to the toxin.

This hypothesis was tested by performing a series of fluorescence quenching experiments with Pet samples at the following temperatures: 4°C, 33°C, 37°C, 41°C, 55°C, and 60°C (Figure 11). A water-soluble quencher, acrylamide, was used and added up to 60 mM. At 4°C acrylamide did not have a significant on Pet suggesting that the tryptophan residues at low temperatures are not exposed to solvent. The levels of quenching increased from 4°C to 33°C and to a greater extent when Pet was incubated at 37°C. Additional quenching did not occur in the temperature range of 37°C to 55°C. Interestingly, at 60°C acrylamide quenching of Pet appeared to be at the same level as 4°C, indicating that Pet is most likely aggregated and the tryptophan residues are inaccessible to acrylamide. The Stern-Volmer (K_{SV}) constants shown in the figure 11 inset represents the quenching efficiency of acrylamide and is plotted as a function of temperature. The K_{SV} values show that maximal quenching occurred around 37°C, physiological temperature, with little variations between 41°C and 55°C. At 60°C there was a considerable decrease in acrylamide quenching possibly due to protein aggregation as well as denaturation. This phenomenon was also observed with the irreversible folding of Pet secondary and tertiary structures (Figure 8B and 10). In addition, the temperature dependent near-UV CD displayed a biphasic dependence on temperature which suggested protein denaturation and

aggregation at higher temperatures; this would most likely inhibit acrylamide access and thus prevent fluorescence quenching.

The acrylamide quenching experiment and near-UV CD shows a consistency of gradual Pet tertiary structure destabilization from 18°C to 40°C, but as depicted by fluorescence spectroscopy a red shift and tryptophan exposure to solvent only occurred at temperatures above 40°C. Collectively, these results again indicate that only subtle alterations to the tertiary structure of Pet occur at physiological temperature. This allows quenching to occur by acrylamide, a water-soluble quencher, but without significant tryptophan exposure. We therefore propose that Pet activates ERAD through hydrophobic residues that are surface exposed without dramatic alterations to the overall structure of the toxin.

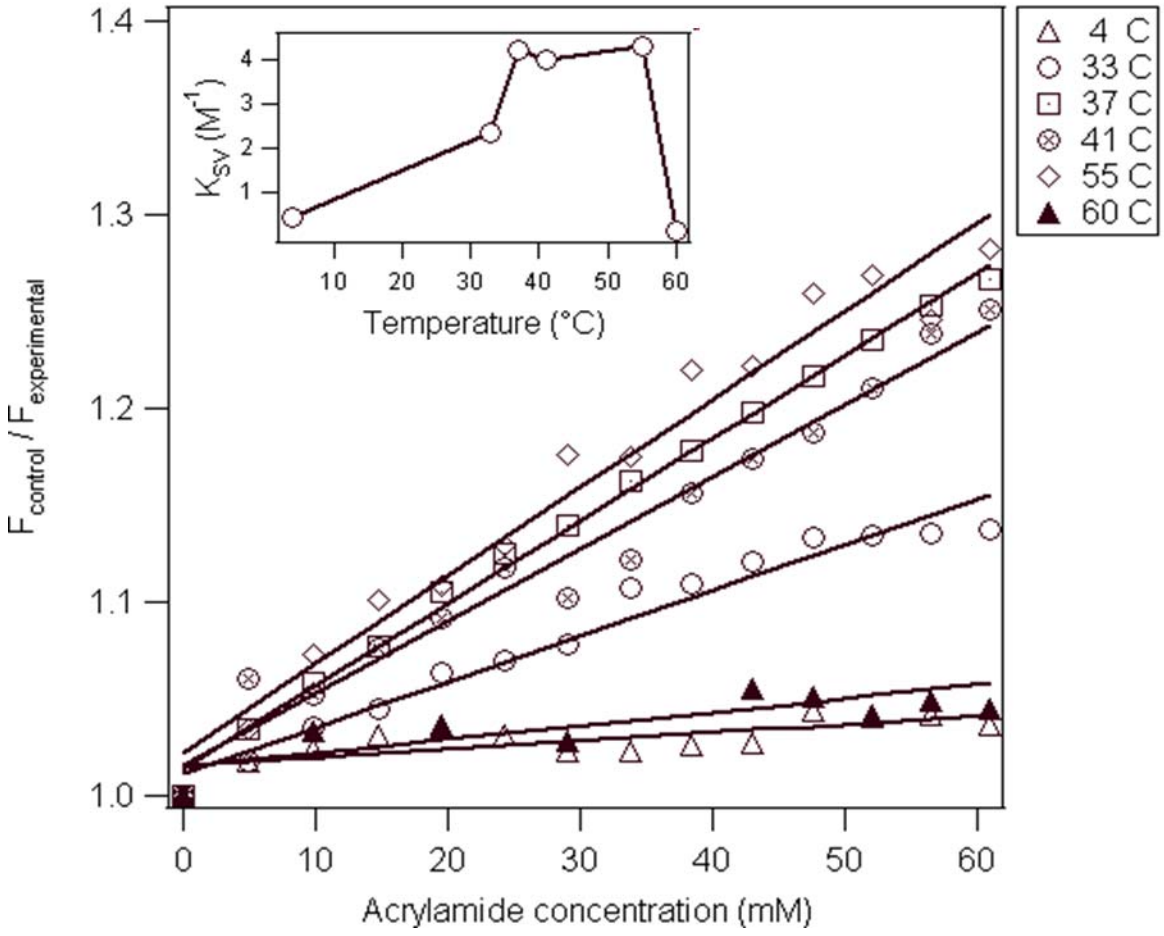

Figure 11: Quenching of Pet Tryptophan Fluorescence

For each indicated temperature, fluorescence spectra were measured with two parallel samples of Pet: one sample in which increasing amounts of acrylamide were added ($F_{experimental}$), and the other sample where an increasing volume of buffer was added ($F_{control}$). The graph represents the ratio ($F_{control} / F_{experimental}$) for each of the corresponding set of samples as a function of acrylamide concentration. The inset displays K_{SV} values as a function of temperature.

The hydrophobic properties of Pet were also demonstrated by another method, a thermolysin protease sensitivity assay (Figure 12). Thermolysin cleaves on the amino-terminal side of the peptide bond at specific hydrophobic residues (valine, alanine, isoleucine, leucine, phenylalanine, and methionine). Protease sensitivity would indicate that Pet contains surface-exposed hydrophobic residues other than the tryptophan residues detected in the fluorescence experiments.

Individual Pet samples were incubated at 4°C, 25°C, 33°C, 37°C, or 41°C for one hour then placed on ice at 4°C where the thermolysin was added to each sample for an additional hour. Since the samples of Pet were pre-incubated at various temperatures, but all thermolysin digestions occurred at 4°C the observed differences in proteolysis are solely due to conformational changes induced by temperature. Samples of Pet that were incubated at 33°C and 37°C were considerably susceptible to thermolysin proteolysis with hardly any toxin remaining. Complete digestion of Pet by thermolysin occurred at 41°C. These results are consistent with CD and fluorescence experiments which show a subtle destabilization of secondary and tertiary structures (Figures 8-9), as well as a more relaxed tertiary structure (Figure 11) around physiological temperature. Interestingly, when Pet was in the presence of an equimolar concentration of α-fodrin it was less susceptible to degradation by thermolysin. The interaction with α-fodrin may have induced conformational changes in Pet that would prevent exposure of hydrophobic residues, but there is also a chance that α-fodrin acted as a competitive inhibitor thus preventing toxin-protease interactions. These possibilities could be differentiated in the future with structure-function methods such as FTIR.

In addition, a protease sensitivity assay with reduced CTA1/2 heterodimer was carried out in order to determine the specificity of the α-fodrin effect for Pet. In the presence of 10 mM

β-mercaptoethanol the heterodimer CTA1/2 was reduced in order to mimic holotoxin disassembly which normally occurs in the ER. It has been demonstrated that reduced CTA1 is sensitive to thermolysin proteolysis at 37°C and 41°C, but displays protease-resistance at lower temperatures (Pande, Scaglione et al. 2007). Moreover, α-fodrin did not have an effect on CTA1 protease activity. This shows the specificity of α-fodrin for Pet in the thermolysin assay.

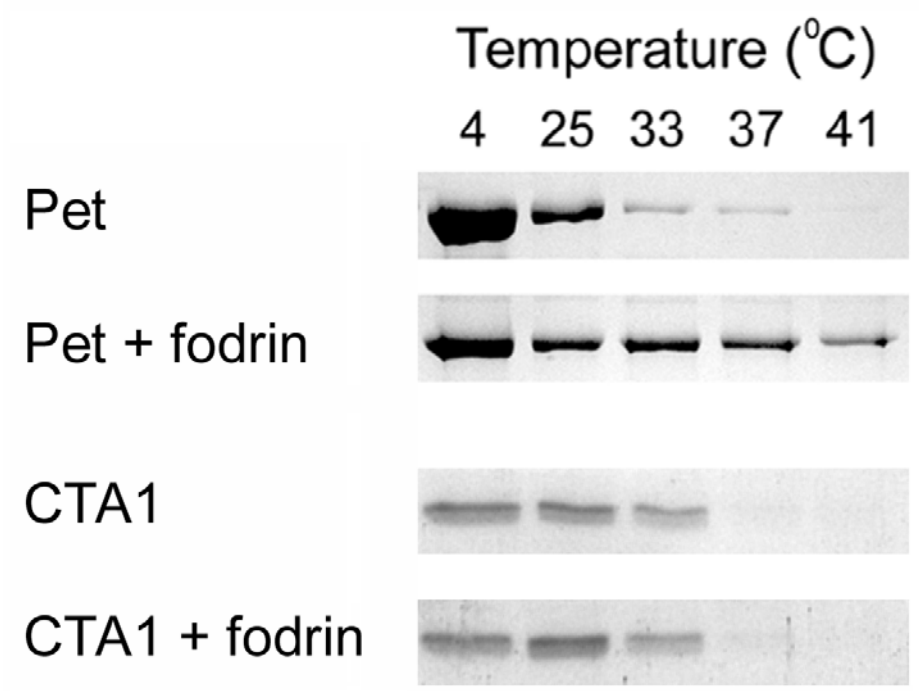

Figure 12: Pet Protease Sensitivity Assay

Pet or the reduced heterodimer CTA1/CTA2 was incubated separately at 4°C, 25°C, 33°C, 37°C, and 41°C for one hour in the presence or absence of α-fodrin. The toxin samples were exposed to thermolysin for one hour at 4°C then resolved by SDS-PAGE with Coomassie staining.

Computer Modeling of Pet Structure

Our data suggest that Pet contains surface-exposed hydrophobic residues at physiological temperature based on the acrylamide quenching experiment and the protease sensitivity assay. Pet has not yet been crystallized, but the crystal structure of another SPATE, hemoglobin protease, has been determined (Otto, Sijbrandi et al. 2005). In order to identify the location of surface-exposed hydrophobic residues, the structure of Pet was modeled using hemoglobin protease as the template. The program, ESyPred3D, from the ExPASy proteomics tools website was utilized to model Pet. Further computer analysis of the Pet structure was used to identify exposed hydrophobic residues that could potentially trigger ERAD (Figure 13). Pet contains seven tryptophan residues, and of those seven, only three (Trp_{274}, Trp_{628}, and Trp_{985}, where numbering starts at the leader sequence) were somewhat solvent-exposed as shown by the space-filling diagram. Of the four remaining tryptophan residues two were hidden within the β-helix (Trp_{403} and Trp_{860}) and the other two were not included in the modeled structure (Trp_{61} and Trp_{642}). The three solvent-exposed tryptophan residues are not likely to activate ERAD due to spatial segregation and only partial exposure to solvent. However, when the residues susceptible to proteolysis by thermolysin were mapped in a space-filling view it showed that there are several solvent-exposed hydrophobic amino acid residues. In particular, one cluster stood out revealing mostly exposed residues including: F_{297}, L_{305}, L_{308}, F_{309}, and I_{310}. Interestingly, these residues are located in an exposed loop that connects the catalytic domain to the β-helix (Figure 13). This stretch of hydrophobic residues could potentially be the site for ERAD activation.

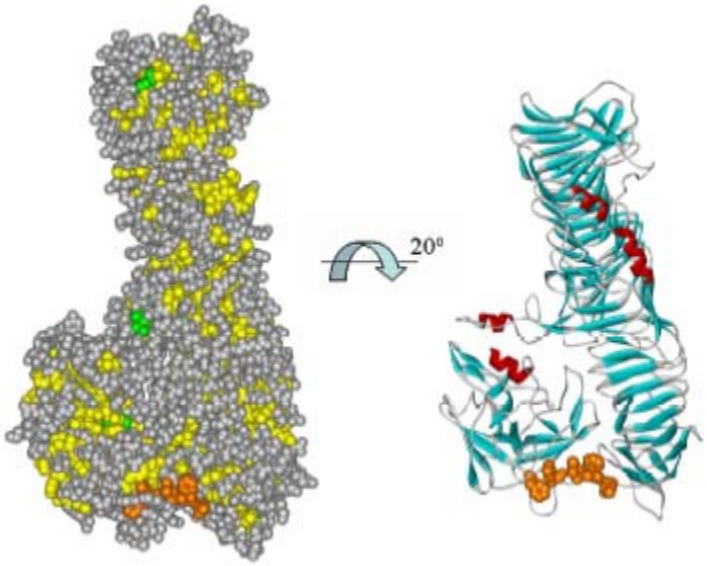

Figure 13: Surface-Exposed Hydrophobic Residues of Modeled Pet

The space-filling diagram of Pet shows tryptophan residues highlighted in green and thermolysin-susceptible amino acid residues in yellow. In order to distinguish the catalytic domain from the β-helix domain in the ribbon structure the space-filling model was rotated on a 20° axis. In both models the highlighted orange residues represent the hydrophobic amino acid residues (F_{297}, L_{305}, L_{308}, F_{309}, and I_{310}) which link the catalytic domain with the β-helix. In the ribbon diagram β-sheets are blue and α-helices are red.

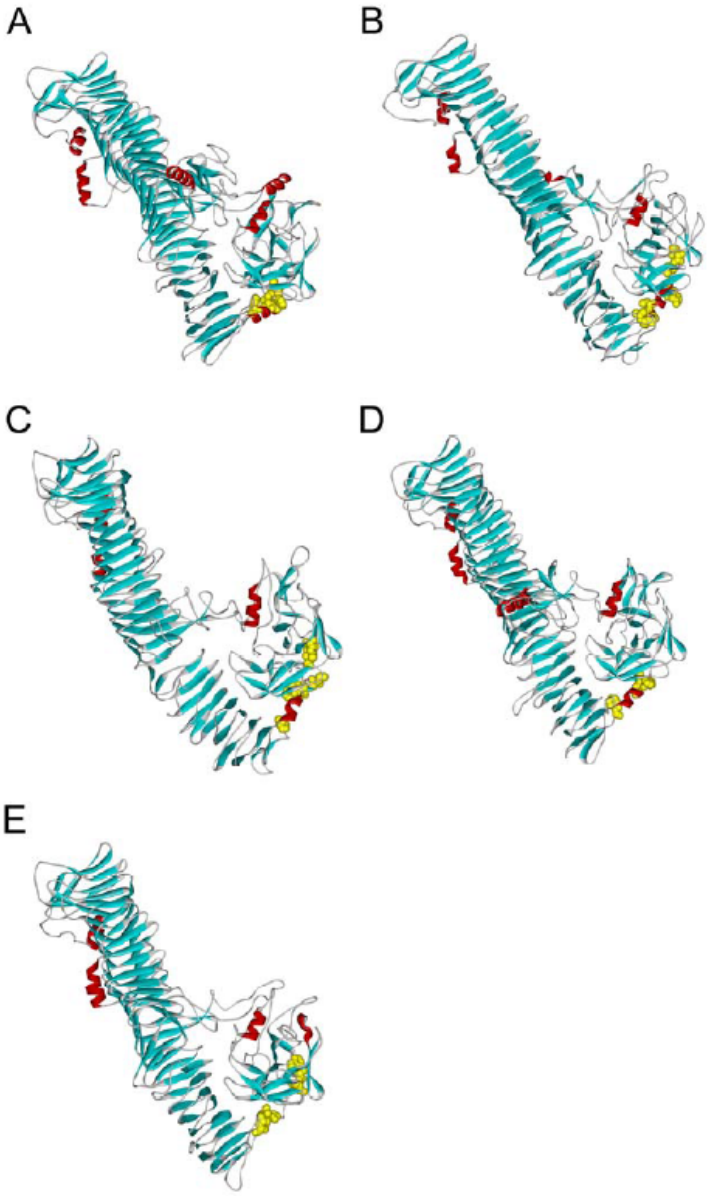

Figure 14: Modeled Structure of Other SPATEs

(A) Hemoglobin protease was used as a template to model the structures of other SPATEs: (B) EspC,(C) EspP, (D) SepA , and (E) the secreted autotransporter of uropathogenic *E. coli* (Sat). Models were generated using ESPred3D from the ExPASy Proteomics tools website. Two other SPATEs (Tsh and Pic) could not be modeled because of limited sequence identity to hemoglobin protease. Amino acid residues in yellow space-filling format are those homologous to the Pet hydrophobic residues (F_{297}, L_{305}, L_{308}, F_{309}, and I_{310}) that are located in the loop linking the β-helix domain to the catalytic domain. B-sheets are highlighted in blue and α-helices are highlighted in red.

CHAPTER FOUR: DISCUSSION

Pet Biogenesis

The folding of auotransporters is thought to be an autonomous process, but it has not been extensively studied. We have shown that the folding of the autotransporter Pet is an inherently inefficient process. Biochemical and biophysical analysis has demonstrated that there are two structurally and functionally distinct variants of Pet. Gel filtration initially indentified two variants, and Western blot analysis confirmed that both fractionated peaks were indeed Pet. Pet peak one did not exist as a dimer or aggregate, which was shown by native gel electrophoresis as well as fluorescence spectroscopy. A toxicity assay showed that Pet peak one did not induce cytopathic effects, while Pet peak two produced the morphological changes to CHO cells. To ensure that the fractionation procedure or the size exclusion buffer did not produce the peak one variant, Pet peak two was rerun on the size exclusion column immediately after the initial fractionation. The resulting elution profile displayed only one peak which corresponded to a properly folded toxin as confirmed through far-UV CD. The unfolded variant is therefore not an artifact of expression.

Structurally, Pet peak one had an unordered protein structure with a minimum of 207 nm and a maximum of about 200 nm. In comparison, Pet peak two was in a folded state with a minimum of 217 nm and a maximum of about 200 nm. From the fluorescence spectroscopy data, a red shift was observed for Pet peak one in comparison to Pet peak two. Pet peak one thus appears to be in a more open conformation than Pet peak two, where the λ_{max} of Pet peak one is about 342 nm and the λ_{max} of Pet peak two is about 327 nm. The fluorescence

spectroscopy data also indicate that Pet peak one did not exist as a dimer or aggregate because, if this were the case, a blue shift would be observed instead of the detected red shift.

To further elucidate the folding characteristics of Pet, the two toxin fractions were immediately collected, denatured, and renatured as separate experiments. One would expect to see a portion of Pet peak one refold into a native conformation, but this was not observed. Interestingly, the denaturaation/renaturation of Pet peak two produced a pool of toxin that was achieved a native confirmation.

Since Pet was purified from the HB101 lab strain of *E .coli*, there was a possibility that a factor present in a pathogenic strain of EAEC was missing from the lab strain. To examine this possibility, Pet was purified from an EAEC strain of *E. coli* and further purified by size exclusion chromatography. The elution profile of Pet from an EAEC strain of *E. coli* showed a single peak, suggesting that the proper folding of Pet required a chaperone present in the EAEC pathogenic strain that was not in the HB101 lab strain. Far-UV CD spectra of the fractionated EAEC sample revealed a single minimum at about 213 nm and a maximum around 200 nm. This is consistent with the CD spectrum of folded Pet peak two from the HB101 lab strain of *E. coli*. Our data indicate that folding of the autotransporter Pet is not a self-sufficient process, and a specific factor such as a chaperone aids the toxin to some extent in achieving an active, native conformation.

Pet ERAD Interactions

After holotoxin disassembly in the ER, the A subunits of certain AB toxins (at physiological temperature) are thermally unstable (Argent, Parrott et al. 2000; Pande, Moe et al. 2006; Pande, Scaglione et al. 2007). The dissociated A subunit at 37° C is in a partially

unfolded state, which identifies it as a misfolded protein and triggers its ERAD-mediated translocation to the cytosol. In comparison, Pet is not an AB toxin and moves from the ER to the cytosol as an intact 104 kDa protein (Navarro-Garcia, Canizalez-Roman et al. 2007). The results of project #2 demonstrated that Pet, at 37°C, is thermally stable and thus exploits ERAD through a mechanism distinct from AB toxins.

At physiological temperature only minor alterations occur to the secondary and tertiary structures of Pet, thus suggesting that Pet can masquerade as a misfolded protein to activate the ERAD mechanism without substantial unfolding observed for toxin A chains. However, the CD, fluorescence quenching, and protease sensitivity assays detected subtle temperature-dependent changes to the structure of Pet. Several surface-exposed hydrophobic residues were identified when the structure of Pet was modeled after Hbp, the only crystallized SPATE. One cluster of these residues were located in an unstructured region of Pet which links the catalytic domain to the β-helix domain, and thus could potentially trigger ERAD.

The width of Pet, from the amino terminus to the β-helix, is about 76 Å, but the pore of the Sec61 membrane pore has a maximum diameter of only 60 Å (Hamman, Chen et al. 1997). Since the diameter of Pet is significantly larger than the pore, an unfolding event or structural rearrangement of Pet must occur for it to reach the cytosol from the ER. Interestingly, Pet contains a linker region, connecting the catalytic domain with the β-helix, which contains several surface-exposed hydrophobic residues. These residues are located in an unstructured area of the toxin. This linker may act as an ERAD to trigger translocation to the cytosol. Chaperones present in the ER may be recruited to this site of hydrophobic residues and facilitate a toxin structural change, since in its native state Pet cannot fit through the Sec61 translocon. We propose that chaperones of the ER pivot the hydrophobic linker

region so that the toxin attains a linear state. However, this would not completely make Pet translocation competent, there is an α-helical motif located just above the catalytic domain in the native conformation of the toxin. This α-helical motif would also reorient due to the disruption of hydrogen bonds present between the loop helix and catalytic domain of Pet. The lack of secondary structure of the putative hinge region suggests that Pet, to a degree, is a flexible toxin. The other SPATEs in Figure 14 appear to contain secondary structure in this linker region, but these toxins do not translocate from the ER, with the exception of secreted autotransporter toxin (Sat) of uropathogenic *E. coli*. Sat, like Pet, acts on the actin cytoskeleton and internalization is required for cytopathic activity to occur (Maroncle, Sivick et al. 2006).

Pet refolding most likely occurs in the cytosol before reaching its target, fodrin. We have shown through refolding experiments the tertiary structure of Pet regain its native conformation after being in a partially unfolded state at 50°C. In addition, our protease sensitivity assay suggests that the interaction taking place between Pet and fodrin may aid in the stabilization of the toxin. This stabilization has also been demonstrated with toxin A chains and their cytosolic targets or other co-factors (Argent, Parrot et al. 2000; Pande, Moe et al. 2006; Pande, Scaglione et al. 2007).

CHAPTER FIVE: CONCLUSION

Autotransporters comprise a diverse family of virulence factors but, are similar in structure. Here, we examined the structure, function, and biogenesis of the autotransporter Pet. We have shown that autotransporter folding is not as self-sufficient as the current model states. Based on the structure of Pet, our data indicate that the toxin has evolved to manipulate host functions to induce cytopathic effects in a manner distinct from ER-translocating AB toxins. Future studies will include identifying the pathogenic-specific factor that aids in proper folding of the autotransporter Pet. Also performing site directed mutagenesis in the surface- exposed loop which connects the catalytic domain with the β-helix.

REFERENCES

Argent, R. H., A. M. Parrott, et al. (2000). "Ribosome-mediated folding of partially unfolded ricin A-chain." J Biol Chem **275**(13): 9263-9.

Bernardi, K.M., M.L. Forster, et al. (2008). "Derlin-1 facilitates the retro-translocation of cholera toxin." Mol Biol Cell **19**(3): 877-84.

Canizalez-Roman, A. and F. Navarro-Garcia (2003). "Fodrin CaM-binding domain cleavage by Pet from enteroaggregative *Escherichia coli* leads to actin cytoskeletal disruption." Mol Microbiol **48**(4): 947-58.

Cantor, C.R., and Schimmel, P. R. (1980) Part II: "Techniques for the study of biological structure and function, in *Biophysical Chemistry*, W.H. Freeman and Co., New York.

Deeks, E. D., J. P. Cook, et al. (2002). "The low lysine content of ricin A chain reduces the risk of proteolytic degradation after translocation from the endoplasmic reticulum to the cytosol." Biochemistry **41**(10): 3405-13.

Ellgaard, L. and A. Helenius (2003). "Quality control in the endoplasmic reticulum." Nat Rev Mol Cell Biol **4**(3): 181-91.

Eslava, C., F. Navarro-Garcia, et al. (1998). "Pet, an autotransporter enterotoxin from enteroaggregative *Escherichia coli*." Infect Immun **66**(7): 3155-63.

Garty, H. and L. G. Palmer (1997). "Epithelial sodium channels: function, structure, and regulation." Physiol Rev **77**(2): 359-96.

Hamman, B.D., J.C. Chen, et al. (1997). "The aqueous pore through the translocon has a diameter of 40-60 Å during cotranslational protein translocation at the ER membrane. Cell **89**: 535-544.

Harrington, S. M., E. G. Dudley, et al. (2006). "Pathogenesis of enteroaggregative *Escherichia coli* infection." FEMS Microbiol Lett **254**(1): 12-8.

Harris, A. S. and J. S. Morrow (1990). "Calmodulin and calcium-dependent protease I coordinately regulate the interaction of fodrin with actin." Proc Natl Acad Sci U S A **87**(8): 3009-13.

Hazes, B. and R. J. Read (1997). "Accumulating evidence suggests that several AB-toxins subvert the endoplasmic reticulum-associated protein degradation pathway to enter target cells." Biochemistry **36**(37): 11051-4.

Henderson, I.R., J. Czeczulin, et al. (1999). "Characterization of Pic, a secreted protease of *Shigella flexneri* and enteroaggregative *Escherichia coli*." Infect Immun **67**(11): 5587-96.

Henderson, I. R., S. Hicks, et al. (1999). "Involvement of the enteroaggregative *Escherichia coli* plasmid-encoded toxin in causing human intestinal damage." Infect Immun **67**(10): 5338-44.

Henderson, I. R. and J. P. Nataro (2001). "Virulence functions of autotransporter proteins." Infect Immun **69**(3): 1231-43.

Henderson, I. R., F. Navarro-Garcia, et al. (2004). "Type V protein secretion pathway: the autotransporter story." Microbiol Mol Biol Rev **68**(4): 692-744.

Henderson, I. R., F. Navarro-Garcia, et al. (1998). "The great escape: structure and function of the autotransporter proteins." Trends Microbiol **6**(9): 370-8.

Jong, W. S., C. M. ten Hagen-Jongman, et al. (2007). "Limited tolerance towards folded elements during secretion of the autotransporter Hbp." Mol Microbiol **63**(5): 1524-36.

Junker, M., C. C. Schuster, et al. (2006). "Pertactin beta-helix folding mechanism suggests common themes for the secretion and folding of autotransporter proteins." Proc Natl Acad Sci U S A **103**(13): 4918-23.

Klauser, T., J. Kramer, et al. (1993). "Characterization of the *Neisseria* Iga beta-core. The essential unit for outer membrane targeting and extracellular protein secretion." J Mol Biol **234**(3): 579-93.

Lambert, C., N. Leonard, et al. (2002). "ESyPred3D: Prediction of proteins 3D structures." Bioinformatics **18**(9): 1250-6.

Lavigne, P., M. P. Crump, et al. (1998). "Insights into the mechanism of heterodimerization from the 1H-NMR solution structure of the c-Myc-Max heterodimeric leucine zipper." J Mol Biol **281**(1): 165-81.

Lord, J. M. and L. M. Roberts (1998). "Toxin entry: retrograde transport through the secretory pathway." J Cell Biol **140**(4): 733-6.

Maroncle, N.M., K.E. Sivick, et al. (2006). Protease activity, secretion, cell entry, cytotoxicity, and cellular targets of secreted autotransporter toxin of uropathogenic *Escherichia coli*." Infect Immun **74**: (6124-6134).

Navarro-Garcia, F., A. Canizalez-Roman, et al. (2007a). "Pet, a non-AB toxin, is transported and translocated into epithelial cells by a retrograde trafficking pathway." Infect Immun **75**(5): 2101-9.

Navarro-Garcia, F., A. Canizalez-Roman, et al. (2001). "Plasmid-encoded toxin of enteroaggregative *Escherichia coli* is internalized by epithelial cells." Infect Immun **69**(2): 1053-60.

Navarro-Garcia, F., A. Canizalez-Roman, et al. (2007b). "Intoxication of epithelial cells by plasmid-encoded toxin requires clathrin-mediated endocytosis." Microbiology **153**(Pt 9): 2828-38.

Navarro-Garcia, F., C. Eslava, et al. (1998). "In vitro effects of a high-molecular-weight heat-labile enterotoxin from enteroaggregative *Escherichia coli*." Infect Immun **66**(7): 3149-54.

Otto, B. R., R. Sijbrandi, et al. (2005). "Crystal structure of hemoglobin protease, a heme binding autotransporter protein from pathogenic *Escherichia coli*." J Biol Chem **280**(17): 17339-45.

Pande, A. H., D. Moe, et al. (2006). "The pertussis toxin S1 subunit is a thermally unstable protein susceptible to degradation by the 20S proteasome." Biochemistry **45**(46): 13734-40.

Pande, A. H., P. Scaglione, et al. (2007). "Conformational instability of the cholera toxin A1 polypeptide." J Mol Biol **374**(4): 1114-28.

Rikihisa, Y., Y. Zhang, et al. (1994). “Inhibition of infection of macrophages with Ehrlichia risticii by cytochalasins, monodansylcadaverine, and taxol.” Ifect Immun **62**(11): 5126-32.

Roberts, L. M. and D. C. Smith (2004). "Ricin: the endoplasmic reticulum connection." Toxicon **44**(5): 469-72.

Romisch, K. (1999). "Surfing the Sec61 channel: bidirectional protein translocation across the ER membrane." J Cell Sci **112 (Pt 23)**: 4185-91.

Romisch, K. (2005). "Endoplasmic reticulum-associated degradation." Annu Rev Cell Dev Biol **21**: 435-56.

Sandvig, K. and B. van Deurs (2002). "Transport of protein toxins into cells: pathways used by ricin, cholera toxin and Shiga toxin." FEBS Lett **529**(1): 49-53.

Sreerama, N., Woody, R.W. (2000). "Circular dichroism of peptides and proteins., in *Circular Dichroism: Principles and Applications*." (Berova, N., Nakanishi, K., and Woody, R. W., Eds) pp 601-620, John Wiley & Sons, Inc., Hoboken, NJ.

Sui, B.Q., P.R. Dutta, et al. (2003). "Intracellular expression of the plasmid-encoded toxin from enteroaggregative *Escherichia coli*." Infect Immun **71**(9): 5364-5370.

Villaseca, J. M., F. Navarro-Garcia, et al. (2000). "Pet toxin from enteroaggregative *Escherichia coli* produces cellular damage associated with fodrin disruption." Infect Immun **68**(10): 5920-7.

Woody, R. W., and Dunker, A.K. (1996). "Aromatic and cysteine side-chain circular dichroism in proteins, in *Circular Dichroism and the Conformational Analysis of Biomolecules*." (Fasman, G.D., Ed.) pp 109-157, Plenum Press, New York and London.

Worthington, Z. E. and N. H. Carbonetti (2007). "Evading the proteasome: absence of lysine residues contributes to pertussis toxin activity by evasion of proteasome degradation." Infect Immun **75**(6): 2946-53.

Zuckerman, J. B., X. Chen, et al. (1999). "Association of the epithelial sodium channel with Apx and alpha-spectrin in A6 renal epithelial cells." J Biol Chem **274**(33): 23286-95.